Review on robot-assisted polishing: status and future trends

Xiaolong Ke[1], Yongheng Yu[1], Kangsen Li[2], Tianyi Wang[3], Bo Zhong[4], Zhenzhong Wang[5], Lingbao Kong[6], Jiang Guo[7], Lei Huang[3], Mourad Idir[3], Chao Liu[8], Chunjin Wang[2]*

1 School of Mechanical and Automotive Engineering, Xiamen University of Technology, Xiamen 361024, China;

2 State Key Laboratory of Ultra-precision Machining Technology, Department of Industrial Systems and Engineering, The Hong Kong Polytechnic University, Hung Hom, Kowloon, Hong Kong, China;

3 National Synchrotron Light Source II (NSLS-II), Brookhaven National Laboratory, PO Box 5000, Upton, NY 11973, USA;

4 Department of Automation, Tsinghua University, Beijing 100084, China;

5 School of Aeronautics and Astronautics, Xiamen University, Xiamen 361005, China;

6 Shanghai Engineering Research Center of Ultra-Precision Optical Manufacturing, School of Information Science and Technology, Fudan University, Shanghai 200438, China;

7 Key Laboratory for Precision and Non-traditional Machining Technology of Ministry of Education, Dalian University of Technology, Dalian 116024, China;

8 College of Engineering and Physical Sciences, Aston University, Birmingham B47ET, UK；

Corresponding author: chunjin.wang@polyu.edu.hk

Abstract: Nowadays, precision components have been extensively used in various industries such as biomedicine, photonics, and optics. To achieve nanometric surface roughness, high-precision polishing is mandatory. Compared with the conventional polishing techniques, the robot-assisted polishing has the advantages of flexible working ranges and low cost. Therefore, it has been more widely deployed in demanding polishing tasks. However, few review articles were found on this topic to provide a general progress on the development of the robot-assisted polishing technology. This paper reviews the recent advancement of the robot-assisted polishing. Firstly, the integration of robots with various polishing techniques is overviewed, followed by the introduction of the research status of constant force control in robot-assisted polishing. Then, the errors in typical robot-assisted polishing systems are analyzed, together with the corresponding compensation methods. At last, the future trends in the development of robot-assisted polishing are discussed. This review is intended as a roadmap for researchers or engineers who are interested in robot-assisted polishing or machining.

Keywords: Polishing; robot-assisted polishing; force control; error compensation; ultra-precision machining.

Contents

1.Introduction

In the 1960s, industrial robots were first employed in the automobile manufacturing industry in the United States. Since then, the repetitive labor works have been gradually replaced by the automated robot-assisted operations. With the rapid development of numerical control and artificial intelligence, the industrial robots have been extensively applied in various industrial fields such as automobile, express logistics, aerospace, and shipbuilding. Robot-assisted manufacturing has thus been extensively applied, which brought the improvement of both the process efficiency and product quality.

Fig.1 presents the statistics from the International Federation of Robotics (IFR) from 2011 through 2020. Compared with Europe and Americas, Asia/Australia currently is the world's largest industrial robot market, with 266,000 newly deployed robots in 2020, which accounted for 71% of new global deployments. From 2015 to 2020, robot installations have increased by a factor of ~11% each year. It is worth noting that China is the largest market for industrial robots in the world. In 2020, the number of installed industrial robots in China exceeded 160,000 units. (Executive Summary World Robotics 2021 Industrial Robots)

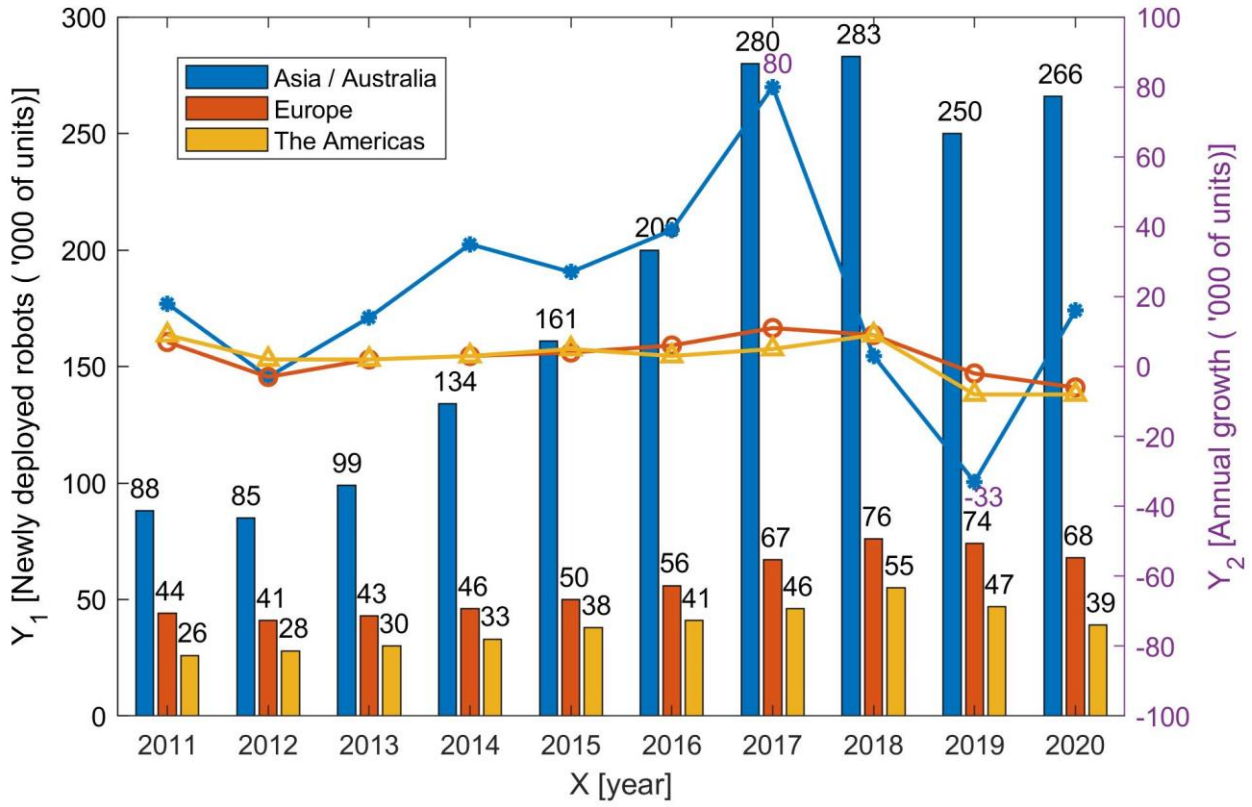

Fig.1 The distribution of global installation of industrial robots from 2011 to 2020(Executive Summary World Robotics 2021 Industrial Robots).

Polishing is a technique which uses a certain machine tool to reduce the final residual errors on the surface of a workpiece through precision-controlled mechanical or chemical processes [1]. Conventionally, polishing was manually done by an artisan based on his/her experience, resulting in unstable surface quality and low efficiency, which could hardly meet the demand for the nanometric

surface quality. Therefore, the manual labor works in polishing have been gradually replaced by the numerically controlled polishing machines and robots [2,3], which effectively improved the polishing efficiency and surface quality. Fig.2 shows some representative polishing machines, including the IRP series bonnet polishing machines developed by the London Optical Laboratory and Zeeko Company [4,5], the ion beam polishing machine jointly launched by NTG Company and IOM Research [6], the magnetorheological polishing machine developed by the University of Rochester and QED Company [7], and the plasma polishing machine model Helios1200 developed by Cranfield University [8].

(a) (b)

(c) (d)

Fig.2 Representative commercialized polishing machines: (a) Bonnet polishing machine IRP1200[5]; (b) Ion beam polishing machine IBF1500[6]; (c) Magnetorheological polishing machine Q22-750[7]; and (d) Plasma polishing machine Helios1200[8].

Although polishing machines have high polishing precision, they are usually expensive. Also, one polishing machine is specifically designed for a certain kind of machine tools. The machine will be fixed once it is built. Any upgrade is always hard and needs massive investments of manpower and financial resources. It is even harder to adapt the existing polishing machine to different machine tools without substantial redesign and redevelopment.

Robots have attracted broader attention in the field of polishing since their vast development in the past few years [9]. Both the polishing efficiency and surface quality have been enhanced by the robot-assisted polishing systems. To achieve high process efficiency without compromising the polishing accuracy, robust pose and path generation algorithms are important [10-17]. Various sensors were employed for monitoring, processing and collected information, and predicting the surface roughness through an intelligent algorithm, determining the stop time of polishing and avoiding excessive polishing [18-23]. Even though the robot-assisted polishing has been widely investigated, many critical issues are still open for further exploration. For example, the motion accuracy (positioning accuracy/positioning repeatability/motion accuracy) of robots is below the practical demand and the stiffness is relatively low, which restrict the application of ultra-precision polishing to the nanometric level. Therefore, the precise calibration of the motion error, robust error compensation

methods, and vibration control are particularly important. This paper serves as the first literature review on the recent research progress in robot-assisted polishing techniques, pointing out the key challenges and summarizing the proven effective resolutions.

The rest of the paper is organized as follows. Section 2 introduces different types of robot-assisted polishing techniques reported in the literature. Section 3 describes recent development of the force control technology in robot-assisted polishing, which is one of the main challenges in robot-assisted polishing. The other key challenges of the robot assisted polishing is the error analysis, modelling and compensation, which is introduced in section 4. Section 5 summarizes this review and gives the outlook of the robot-assisted polishing.

2.Various kinds of robot-assisted polishing

A 4 - 6 axis industrial robot is often utilized as the principal part within a robot-assisted polishing system. The machine tool, as shown in Fig.3, is usually installed on the flange at the end of the robotic arm. Compared with the conventional polishing machines, a robotic system has two inherent advantages. First, unlike the linear feed axis of machine tools, industrial robots have more Degrees of Freedoms (DOFs) thanks to the adopted rotating joints. Thus, it is easy to traverse any position in the processing space and obtain the required processing pose. Second, it is cost effective, and the development cycle is short since industrial robots are standardized and only the machine tool module needs to be developed.

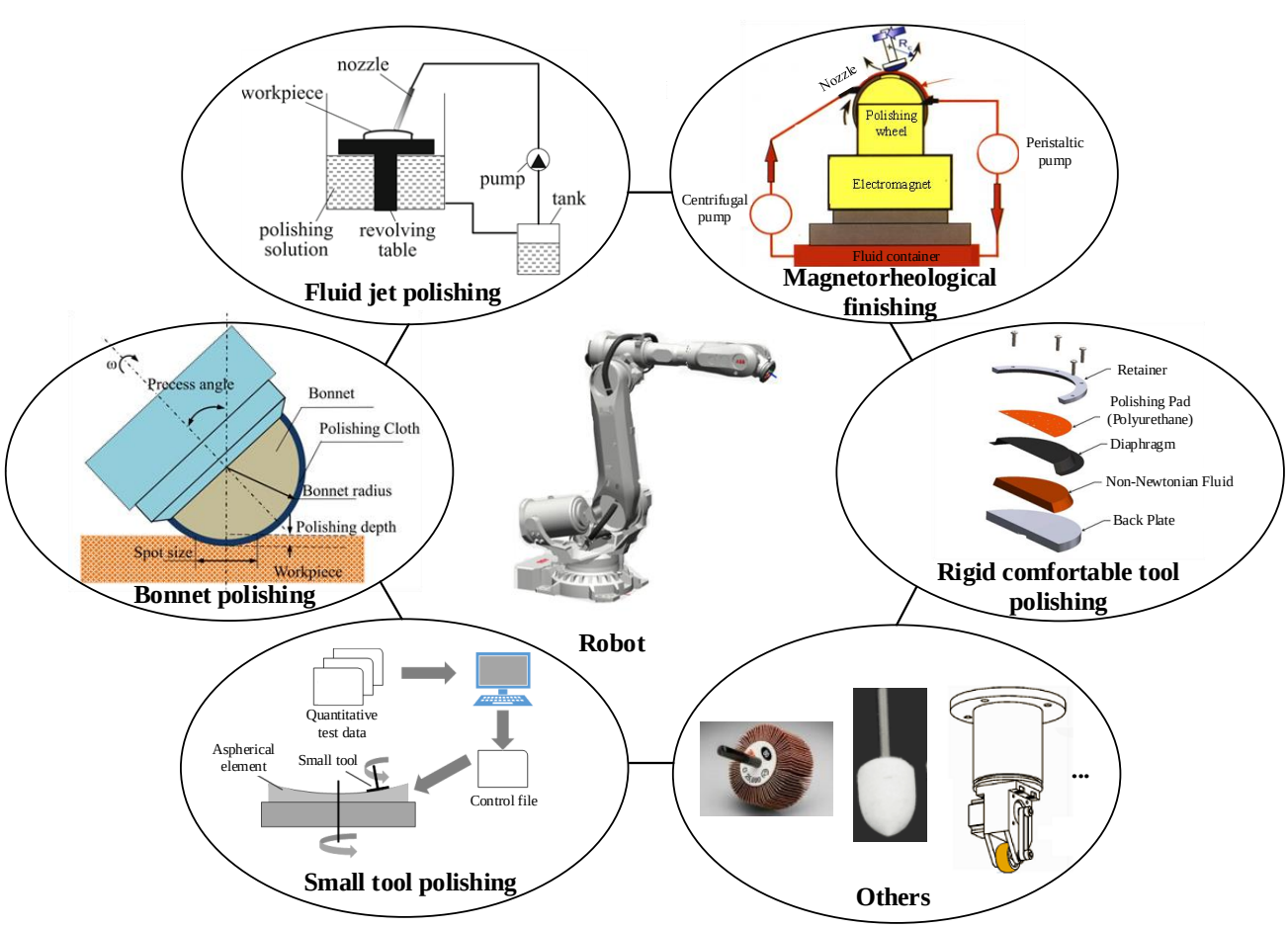

Fig.3 Various kinds of robot-assisted polishing techniques.(Refer to Fig.4, Fig.8, Fig.10, Fig.13, Fig.15 and Fig.18 for details)

As shown in Fig.3, robot-assisted polishing systems have been used in various precision polishing techniques such as small tool polishing (STP), bonnet polishing (BP), fluid jet polishing (FJP), magnetorheological finishing (MRF), and rigid comfortable (RC) tool polishing. In the rest of this section, the representative applications of robot-assisted polishing in each of the techniques are introduced.

2.1 Robot-assisted STP

STP technique has been widely employed in the processing of aspheric surfaces [24,25]. Rupp et al. firstly proposed the concept of Computer Controlled Optical Surface (CCOS), and conducted in-depth research on the material removal mechanism, material removal model and dwell time.

Fig.4 schematically illustrates the principle of CCOS. It suggests that the surface data of the workpiece can be calculated through STP, and a polishing tool that is usually less than 1/5 of the diameter of the workpiece is used. The precise control of material removal is realized by computer-controlled polishing pressure, dwell time, and other parameters of the small tool.

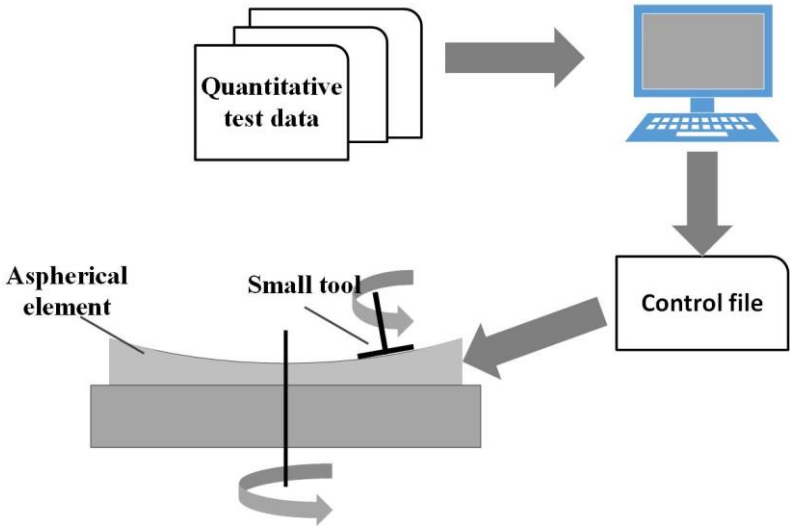

Fig.4 Schematic diagram of CCOS.

Following the development of robotic technology, many researchers combined STP with industrial robots to carry out the polishing tasks. As shown in Fig.5, the control system was integrated into Zeeko tool-path generation software to study the tool wear and optimal spindle speed[26-28]. The robot was used for rough polishing between grinding and corrective polishing to shorten the manufacturing time of optical components.

(a) (b)

Fig.5 (a) Photograph of 3.05m and 2.55m robots, and (b) photograph of 1.8m robots and Zeeko IRP600 machines[26].

The robot-assisted polishing experiments were successfully carried out on glass by taking the advantages of industrial robots such as high flexibility and large working area[29]. The material removal experiments during grinding and polishing were performed on a robotic platform, as shown in Fig.6 (a)and (b), to extract the tool influence function (TIF) in grinding and polishing and study the stability of the TIF. The experimental results demonstrated that the robotic polishing system could produce Gaussian-like TIFs with good stability， as shown in Fig.6 (c).

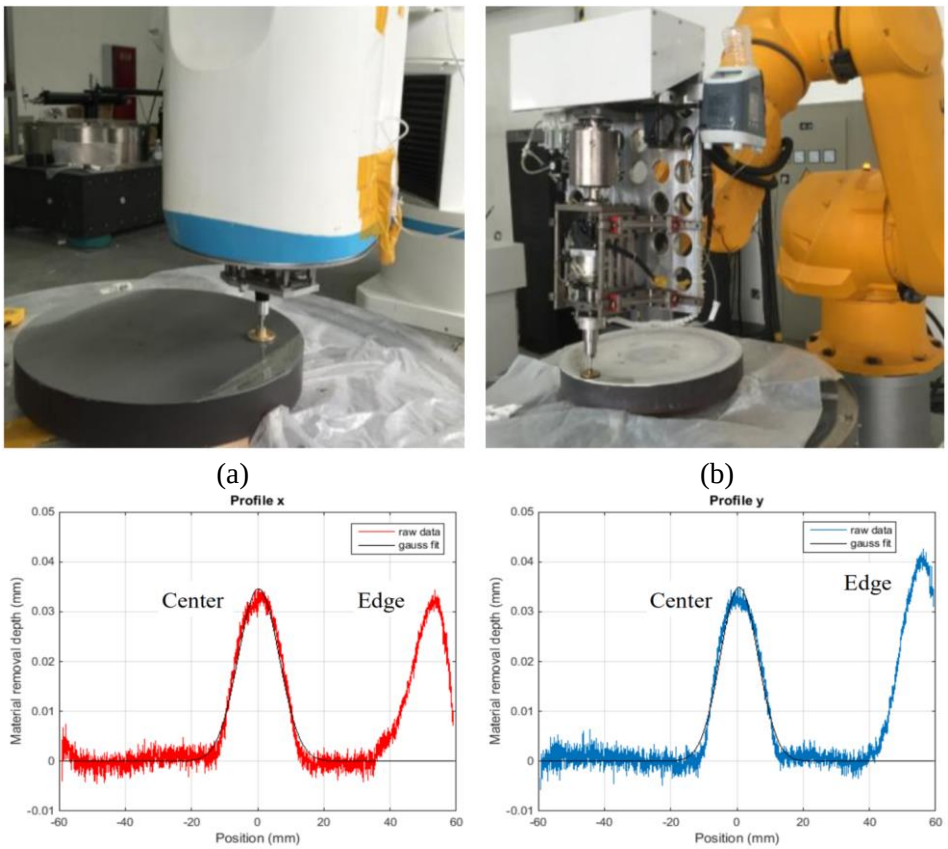

(c)

Fig.6 Photographs of (a) a robot assisted grinding system, (b) a robot-assisted polishing system and (c) TIF in griding and polishing[29].

As shown in Fig.7, Lin et al. [30] proposed the center-inlet computer-controlled polishing (CCCP) technology on the basis of STP, and developed a five-DOFs robotic polishing system shown in Fig.7. The polishing slurry was supplied by the central hole of the polishing tool to improve its utilization efficiency. The flexible coupling was used to keep the polishing tool parallel to the surface of the tool during the polishing process. The quartz glass of the planetary motion trajectory pair was polished to reduce the roughness within the range from 0.1 um to 1.6 nm. The experimental results suggested that CCCP obtained a higher material removal rate and a more stable TIF than those general CCOS techniques.

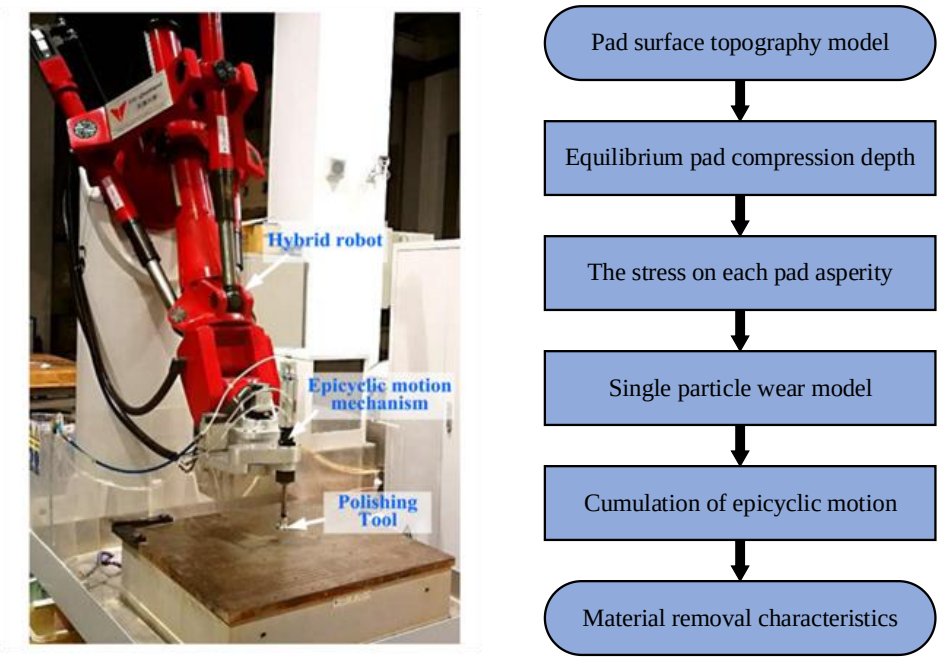

Fig.7 (a) Experimental setup of the robotic polishing system and (b) flowchart of the theoretical modeling process for CCCP[30].

Liu et al. [31] combined STP with a six-axis industrial robot to process two silicon carbide (SiC) aspheric mirrors. After grinding and polishing, the final shape error of the primary mirror was improved from 0.2 mm root mean square (RMS) to 11.4 nm RMS, and the final shape error of the triple mirror was improved from 0.08 mm RMS to 12.1 nm RMS. The experimental results indicated that the robotic polishing system can be applied to process aspheric mirrors. By controlling the tool parameters of CCOS, Wang et al. [10] studied the relationship among the internal coordinate systems of a robot, and established the component coordinate system for optical design and the coordinate system for actual processing. An algorithm governing coordinate transformations was provided. As shown in the experiment, the residual errors of the robotic and the conventional CNC polishing machine reached of 9.83 nm RMS and 7.26 nm RMS, respectively, which proved that the robotic and CNC polishing machines achieved similar material removal rates and surface qualities under the same tool parameters. A deep learning algorithm with feature selection capability was proposed by Yu et al. [32] It learned the polishing parameters from both the simulated samples and actual samples, and established a deep neural network. Based on the learned parameters, the material removal depth of the

test sample was estimated, and the error between the estimated and actual material removal depth was calculated.

With the development of STP and industrial robots, the polishing efficiency has been greatly improved. However, STP belongs to contact-based polishing methods, and the tool is usually in flat disk shape with less flexibility, which has the drawbacks of tool wear and low adaptability to complex surfaces.

2.2 Robot-assisted BP

To compensate for the problems of the STP, BP was invented at the Optical Science Laboratory of University College London, UK. It had soon been commercialized and widely used in the field of optical manufacturing by Zeeko in the UK. As shown in Fig.8, a flexible spherical bonnet is adopted and compressed to the target surface. A unique precession moving method is applied in such flexible bonnet polishing, which combines the rotation and revolution to achieve a messy surface texture. The precession angle can effectively avoid the unexpected "M"-shaped TIF caused by the zero velocity at the center point and form a more favorable Gaussian-like TIF.

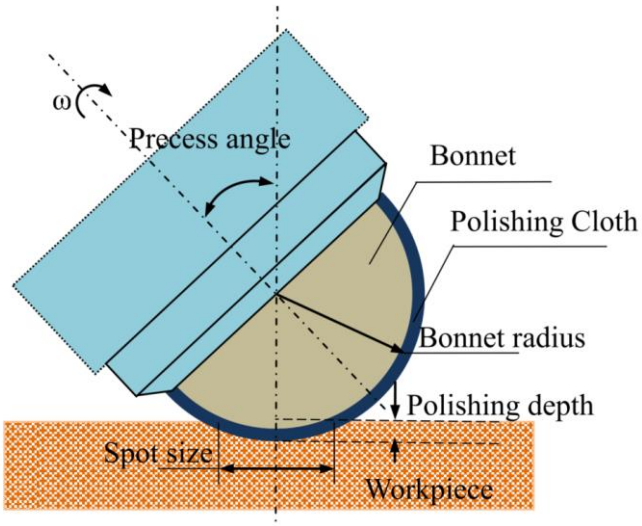

Fig.8 The schematic diagram of BP [33].

Walker et al. [34] firstly proposed the concept of the BP, and carried out extensive experimental research in the early stages of the development of BP technology. It was claimed that a continuous precession could result in a nearly Gaussian TIF, and multi-step precessions could improve the surface quality [35,36]. Some systematic studies were carried out subsequently, including the TIF of BP [37,38], the pseudo-random path algorithm [39] for restraining the mid-spatial frequency (MSF) error, the tool-lift algorithm for edge effect suppression [40], and the grolishing method for pre-polishing [41]. Wang [42] and Pan [43] established the TIF model for BP. Zhong et al. [44] studied the effects of surface curvature on the contact area between the bonnet and the workpiece, and established a time-varying TIF model. Cao et al. [33,45] explored the multi-scale material removal characteristics of BP to predict the material removal. Zhong et al. [46] investigated the effect of polishing pad conditions on removal characteristics. Wang et al. [47,48] designed a semirigid bonnet tool, which not only inherited the flexibility of ordinary bonnet tools, but also obtained higher stiffness and material removal rate.

Pan et al. [49] built a robot-assisted BP system (RABPS) as shown in Fig.9, and its static stiffness model was also built based on the Denavit-Hartenberg (D-H) method and compliance matrix. By combining the static stiffness model and the force analysis results, a new index of the normal stiffness coefficient (NSC) was proposed to evaluate the working stiffness of the RABPS. The experimental result indicated that the evolution of the NSC values was consistent with the actual normal force value, whereas the NSC could be used to effectively evaluate the working stiffness of RABPS, and the working stiffness of RABPS was significantly affected by the working posture.

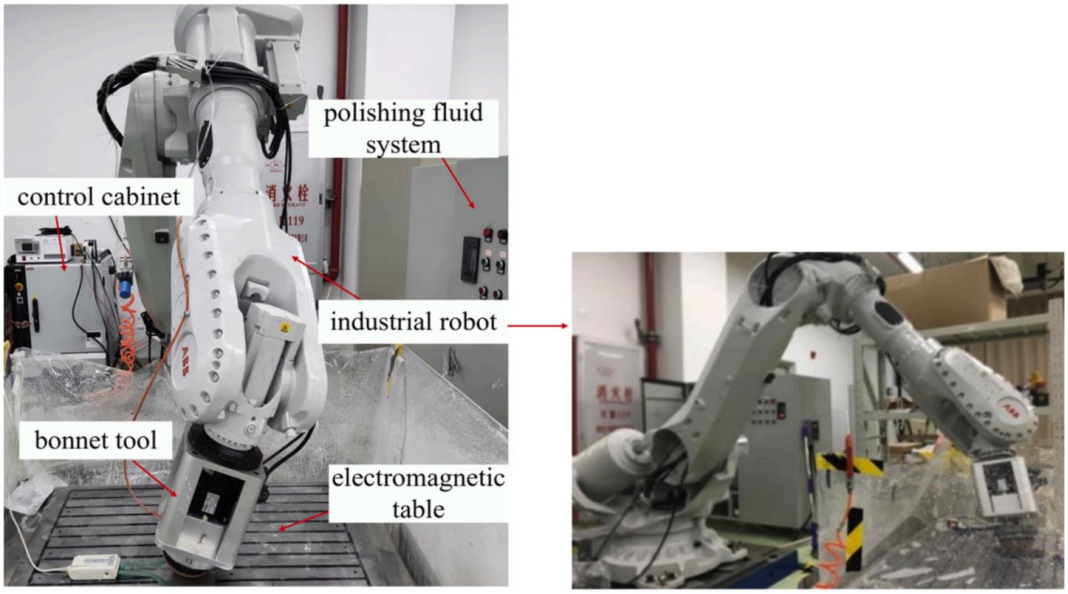

Fig.9 The photographs of Robotic BP system [49].

Zhong et al. [50,51] used robot-assisted BP for precision polishing of large aspheric surfaces, and established a robot-based precession control model. Based on this model, a new motion error compensation method was proposed. The robot motion error was evaluated by the machining error, and the operating parameters of robotic system were adjusted by compensating the machining trajectory error. The experimental results showed that after error compensation, the motion error in the range of 400 mm × 400 mm was reduced by 83%, and this method could effectively improve the precision of aspheric surface pre-polishing. Qin et al. [52] studied the collision detection of multi-robot bonnet polishing. The bounding boxes were used in the collision model so that the collision detection problem was simplified as finding the intersections among bounding boxes.

Due to the flexibility of a bonnet tool, it can be easily adapted to the variable curvatures of a mold surface by controlling the air pressure in the bonnet. Added with the robot, the polishing path and the posture of the polishing tool can be easily regulated. Thus, the robot-assisted BP is suitable for controlling both the texture and from of a workpiece surface. Ji et al. designed and applied a robotic BP system to mold polishing [53]. The experimental process and results showed that the robot-assisted BP system had better stability, higher polishing efficiency, and better surface quality than the conventional mold polishing methods.

Bonnet polishing is a competitive polishing method. The flexible bonnet can make it to well fit to the complex surface shapes. BP also has relatively high polishing efficiency accuracy compared

with STP. It now has been widely used in the polishing of optical molds, freeform components, and even telescope mirrors.

2. 3 Robot-assisted FJP

FJP [54-56] is an energy-beam polishing technology which is based on the abrasive water jet. As shown in Fig.10, after the abrasive and the carrier liquid are fully stirred and uniformly mixed, the polishing slurry is pressurized and sprayed to the workpiece surface through the nozzle to form a jet, under which the material located at the topmost surface is removed by the high-speed movement of the abrasive particles. Thanks to the high flexibility of the water jet, this method is suitable for workpieces with various complex surface shapes with no edge effects. However, the processing efficiency is extremely low due to the small TIF size. Hence, Wang et al. [57] developed the multi-jet polishing (MJP) method to improve the material removal rate. Subsequently, a kind of curvature-adaptive MJP (CAMJP) was also developed to effectively improve the polishing accuracy on free-form surfaces[58].

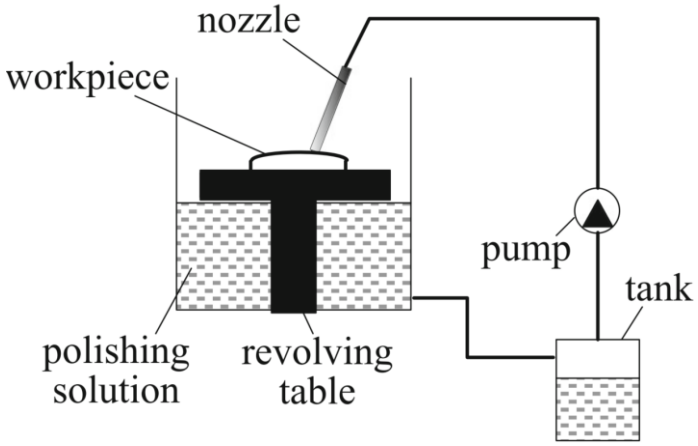

Fig.10 The schematic of the principle of FJP [54].

The combination of FJP and robotic technology makes FJP more flexible and easier to work in various applications. Lv et al. [59] adopted the discrete phase method and computational fluid dynamics (CFD) to simulate the flow field in ultrasonic-assisted abrasive waterjet machining, and designed a robotic ultrasonic-assisted waterjet device as shown in Fig.11. The vibration of the workpiece was simulated by the dynamic mesh method. The effect of ultrasonic vibration on pressure and velocity distributions was investigated in detail, while the influences of particle impact parameters were also revealed. The experimental results showed that the introduction of ultrasonic vibration improved the erosion rate of the abrasive water jet.

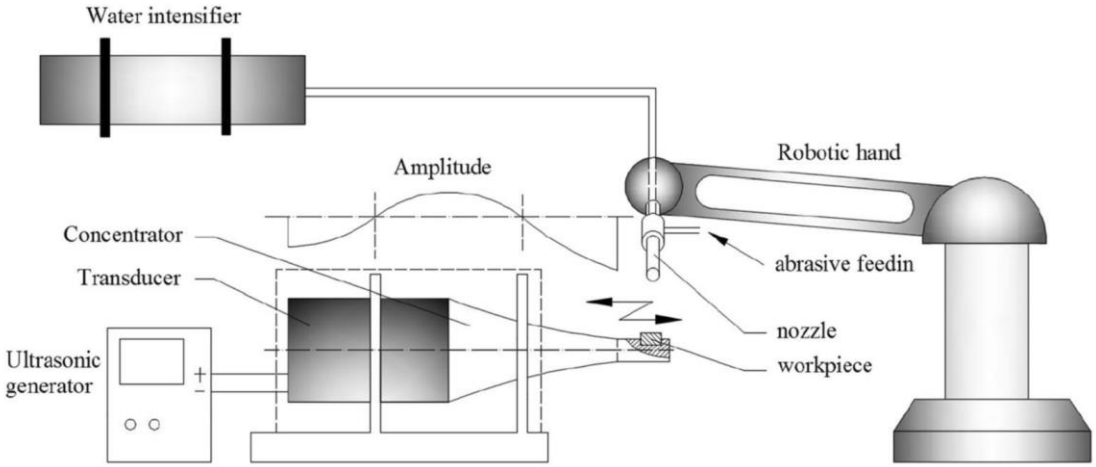

Fig.11 The schematic diagram of robot ultrasonic-assisted water jet device[59].

Hou et al. [60] designed a robot-assisted, abrasive water jet polishing system, which greatly improved the working range of the abrasive water jet. Integrating a robot provided the advantages of simple structure and flexible movement, which could be used to process complex 3D workpieces. Wang et al. [61] investigated the effect of different process parameters including jet impinging angle, stand-off distance, fluid pressure, abrasive particle size on the removal rate, removal depth, and surface roughness of Aluminum nitride (AlN) ceramic materials through single factor experiments. Subsequently, the ultrasonic torsional vibration was conducted on the processing of the workpiece [62], and the process parameters of ultrasonic torsional vibration-assisted abrasive water jet polishing were further optimized by orthogonal experiments. The effect of ultrasonic torsional vibration in abrasive water jet polishing was studied. Experiments were carried out using a robot. As shown in Fig.12, the application of ultrasonic torsional vibration could affect the movement of abrasive particles which could increase the critical depth of ceramic materials and improve the surface quality.

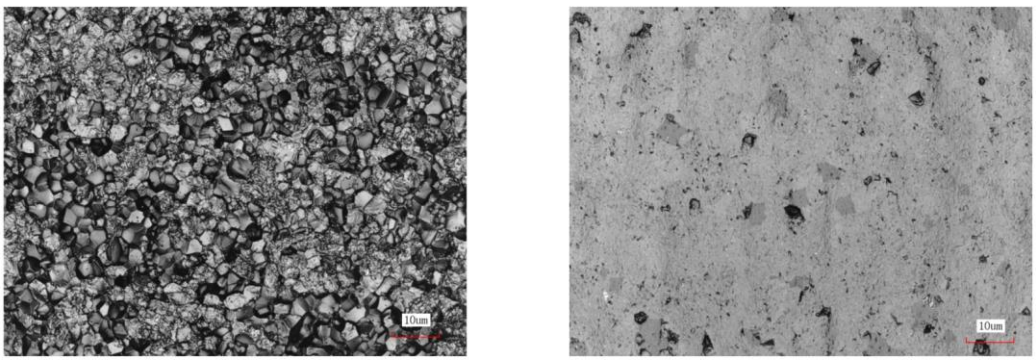

(a) (b)

Fig.12 Surface morphologies of an AlN ceramic: (a) original surface and (b) polished surface [62].

FJP has its unique advantages over BP and STP, such as no thermal effects during polishing, high accuracy, high adaptability to complex surfaces, etc. However, the polishing efficiency is quite low, and the stability of the slurry has a significant influence on the polishing quality, leading to a tight requirement of the high-pressure pump. Also, the valve inside the pump may wear out easily if large particle sizes are used.

2.4 Robot-assisted MRF

MRF uses the rheological properties of the slurry with magnetic materials under the effect of a magnetic field [63,64]. As shown in Fig.13, the magnetorheological fluid is firstly sprayed onto the surface of the polishing wheel through the nozzle, and then cyclically brought into the polishing area by the polishing wheel. A high-strength gradient magnetic field is generated within this region, and the magnetorheological fluid serves as a visco-plastic Bingham medium under the action of the magnetic field. Among them, the magnetic particles are well-arranged along the direction of the magnetic field to form a ribbon, and the abrasive particles are squeezed to the top of the lower magnetic field because of lack of magnetism, thereby forming a flexible polishing film. When the distance between the flexible polishing film and the surface of the polished workpiece is relatively close, a larger shear force can be produced within the magnetorheological fluid, resulting in material removal and generation of inverted D-shaped TIF. After the magnetorheological fluid leaves the magnetic field, it becomes a flowing liquid again and enters the magnetorheological fluid container through a peristaltic pump to realize recycling.

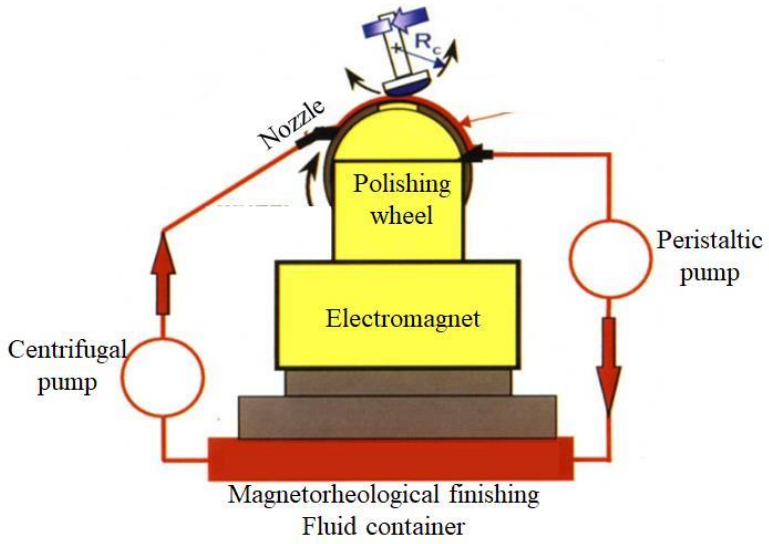

Fig.13 The schematic diagram of principle of MRF[65].

Compared with the conventional MRF machines, robot-assisted MRF methods are more flexible and cost-effective. Fig.14 shows the schematic of MRF combined with a robot [66,67]. A specially designed MRF module is integrated into the six-axis industrial robot. Using this system, a 1000 mm × 470 mm, SiC off-axis aspheric mirrors was successfully processed. The surface accuracy was reduced from 45.76 nm RMS to 22.78 nm RMS after several cycles of iterative polishing.

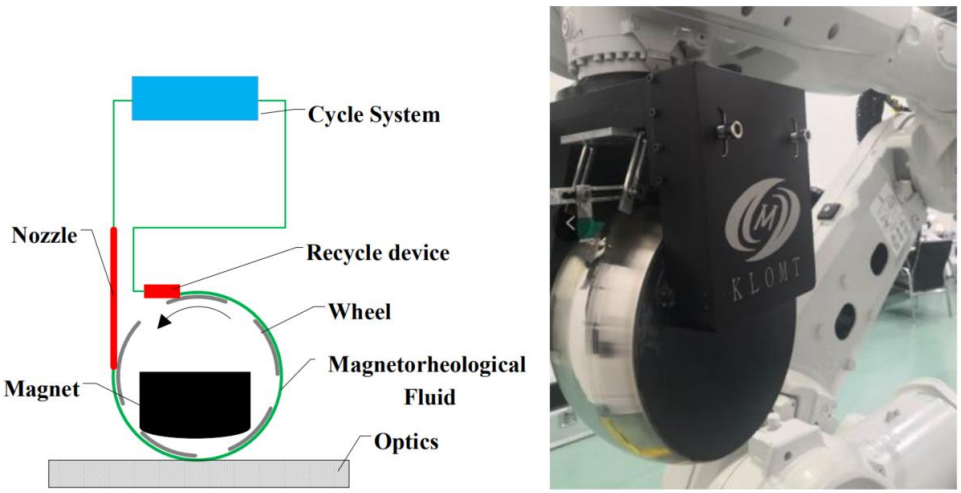

Fig.14 The schematic diagram of a robotic MRF[67].

Although MRF belongs to contact-based polishing, the subsurface damage of the workpiece surface is quite small thanks to its tangential material removal. Moreover, the magnetic ribbon is generated to replace the polishing pad during MRF, which is beneficial to obtaining stable TIF to implement high polishing accuracy. Nevertheless, it still have some drawbacks such as the material limitations, expensive price of the MRF slurry, and relatively low material removal rate.

2. 5 Robot-assisted RC polishing

Kim et al. [68] designed an RC polishing tool using the non-Newtonian fluid for the polishing large telescope mirrors. As shown in Fig.15, the RC tool is composed of a backing plate, non-Newtonian fluid, rubber diaphragm, polishing pad, and retainer. Silly putty is used for filling (Silly putty is a non-Newtonian fluid, which exhibits the fluidity of a liquid when a stable stress is applied; it has the rigidity of a solid when a high-frequency stress is applied). It was experimentally verified that the RC polishing tool had a high removal rate when used as a rigid tool. However, it has not been quantitatively proved that the tool adapts to the slowly changing workpiece curvature.

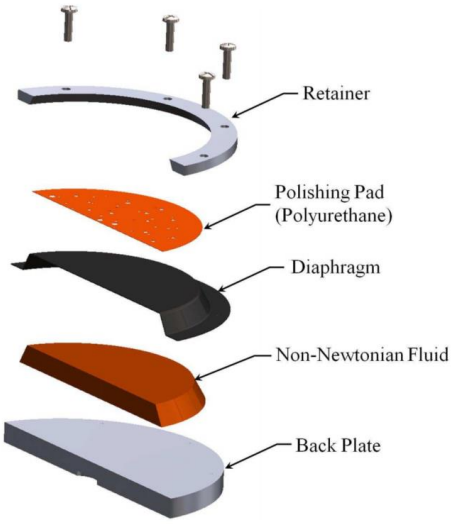

Fig.15 Schematic of the structure of a RC tool[68].

Li et al. [69] built a robot-assisted RC polishing system as presented in Fig.16. After polishing of the 400 mm aluminum mirror, its surface roughness reached ~5 nm Sa as shown in Fig.17, in which the MSF error was effectively suppressed. In addition, Walker et al. [70] introduced a planetary polishing path to further suppress the MSF and high-spatial frequency (HSF) errors, and after polishing, the Sa and Sq values reached 2.9 nm, and 4.88 nm, respectively.

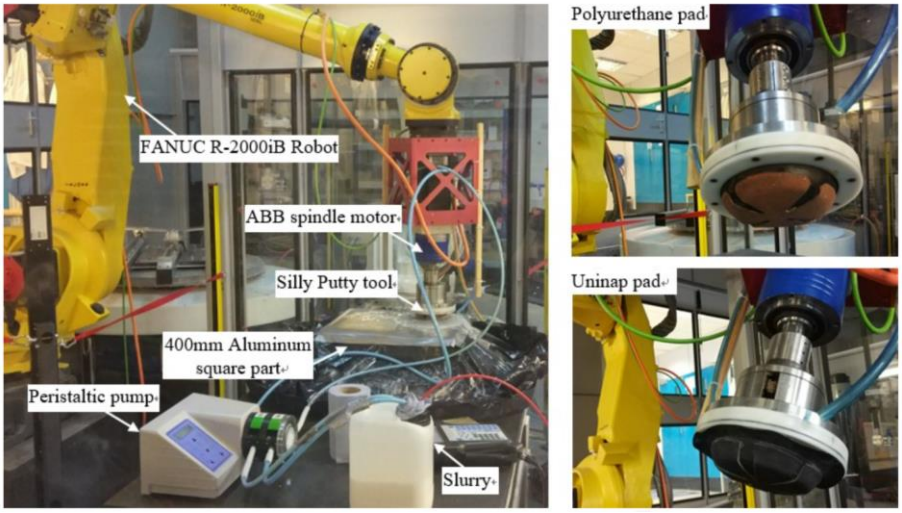

Fig.16 Photographs of robotic RC polishing system[69].

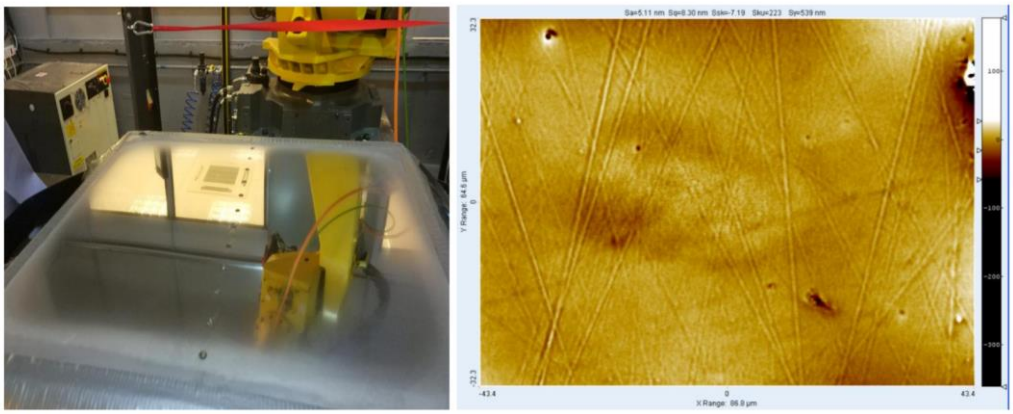

(a) (b)

Fig.17 (a) Surface quality after processing and (b) white light interferometer micrograph of texture showing ~ 5nm Sa [69].

RC polishing tools have strong rigidity and high removal efficiency when the speed is high, while good flexibility is achieved when the speed is low. However, tool interference problems will happen when polishing highly curved or freeform surfaces.

2.6 Others

In addition to the several common polishing methods mentioned above, many other polishing

methods are well used in robot-assisted polishing. Such as wheel polishing, belt polishing, etc. Although these robot-assisted polishing methods have limited polishing accuracy, they have been widely used in industrial applications.

Zhang et al.[71] combined industrial robot and abrasive cloth wheel to achieve precise polishing. Experimental results showed that the flexible adaptive trajectory planning algorithm increased the total polishing efficiency by nearly 9.4%, the surface line roughness of the edge Ra≤0.2μm , and the surface line roughness of the convex and concave of the blade Ra ≤0.3μm. As shown in Fig.18, Wang et al.[72] used robot wheel polishing to improve the surface quality of the NiP and Cu coating. After polishing, the surface accuracy achieved 0.015λ(RMS, λ=632.8nm).

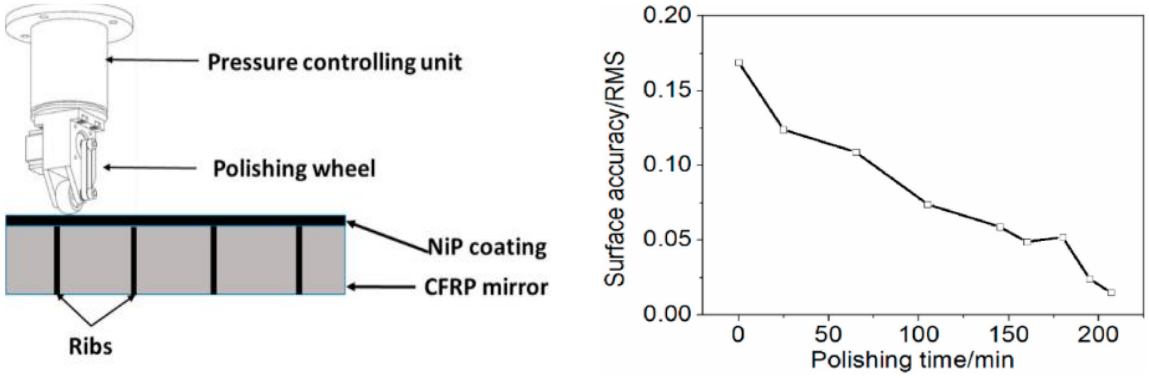

(a) (b)

Fig.18 (a) Robot-arm wheel polishing process of 100mm CFRP mirror and (b) convergence process of surface accuracy[72].

Robotic belt polishing can improve the surface quality of aero-engine blades efficiently. The blade belt polishing process is shown in Fig.19. Guo et al.[73] combined grey correlation analysis and the Taguchi method, to obtain the optimized polishing parameters, and the material removal rate was increased by 16.11%. Xiao et al.[74] proposed an integrated polishing method that combined bob polishing and belt polishing. After polishing, the defects and transition region of knife milling were completely eliminated.

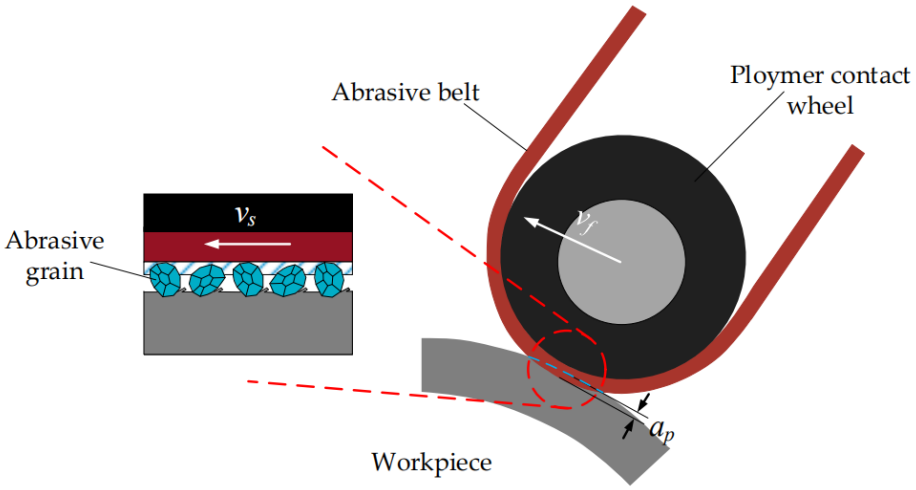

Fig.19 Schematic diagram of the blade belt polishing process[73].

Chong et al. [75].investigated the stability of hybrid mobile robot for the polishing of large blades. As shown in Fig.20, the robot is consisted of an automated guided vehicle (AGV), a two-degree-of-

freedom hybrid module and a 1T2R parallel module. The position movement was regulated by the AGV and the two-degree-of-freedom hybrid module, and the direction of the polishing tool was adjusted by the 1T2R module.

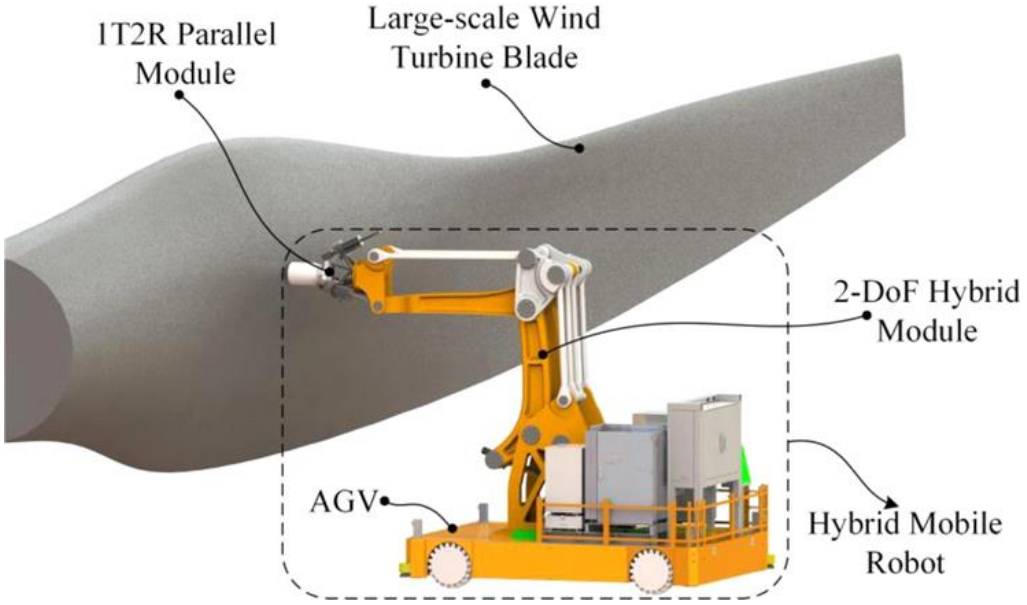

Fig.20 The schematic diagram of hybrid mobile robot polishing system [75].

3. Robot-assisted polishing force control technology

In line with Section 2, the current robot-assisted polishing is mostly integrated into the contact-based mechanical polishing techniques. The polishing force of the polishing process directly affects the material removal rate. Therefore, most of the present methods with constant force control are used to achieve uniform polishing of complex surfaces. This section introduces the current research progress of constant force control of robot-assisted polishing in detail, including passive compliance control and active compliance control two parts.

Preston function has been widely used in the modelling of material removal in mechanical polishing [76] as

$$\frac{dz}{dt} = kpv, \tag{1}$$

where dz/dt is the material removal depth per second; k is the Preston coefficient, which is usually a constant. v and p are the relative polishing velocity and pressure at this point, respectively. The material removal rate produced by a polishing tool at a certain point on the workpiece surface is proportional to the product of the relative velocity at that point and the contact pressure. As shown in Fig.21, under the same conditions, the amount of polishing removal can be controlled by controlling the polishing force, to achieve deterministic polishing.

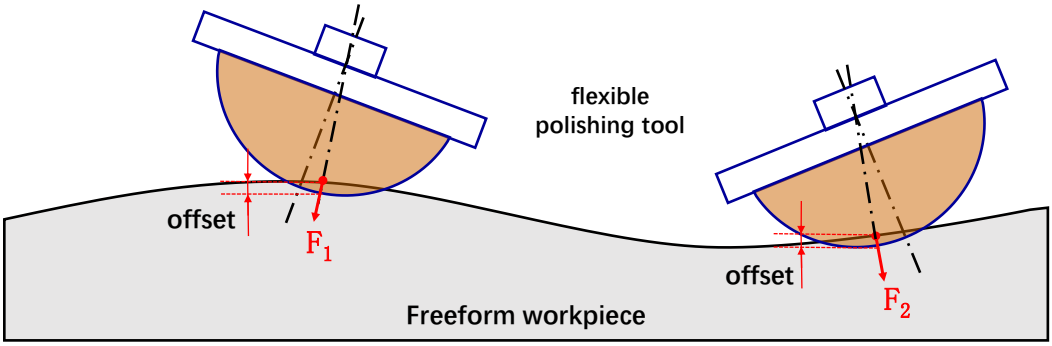

Fig.21 The schematic diagram of robot-assisted polishing force control.

Niwa et al.[77] studied the relationships between polishing pressure and polishing force and material removal rate. It was found to follow an exponential trend and the friction coefficient would be enhanced with the increase of polishing pressure. Based on these findings, the material removal rate could be estimated. Zhang et al. [78] studied the problem of material removal during polishing with spherical polishing tools. They assumed that the pressure distribution between the tool and the contact surface was a Hertzian distribution and proposed a method for calculating the material removal profile. Using the PUMA robot, a series of experiments were carried out on polishing force, effective contact area (divided into convex and concave), spindle speed, feed speed, and polishing tool material. The material removal depth was proportional to the 2/3 power of the polishing force, to the 1/3 power of the contact radius, proportional to the spindle speed, and inversely proportional to the hardness and feed rate. Wan et al. [79] analyzed the generation mechanism of the polishing pad wear, which established an effective model to describe polishing pad wear during optical polishing. The relationship between pad surface shape, movement speed and dwell time was also analyzed. A material removal model of valve cover polishing robot was established[80] based on the Preston equation and the linear velocity distribution and contact stress distribution in circular contact area between flexible polishing tool and die. Polishing pressure directly affects the amount of material removal, as well as the surface shape after polishing. It is of great importance to precisely control the contact force between the tool and the workpiece [81,82]. When the robot is in contact with the workpiece, the end of the robot actively or passively adjusts the changes in the force or torque it receives [83,84]. This control process is called robot compliance control.

In this paper, the compliant control is divided into passive and active compliance control, and introduced in the following sections.

3.1 Passive compliance control

Passive compliance means that the robot can absorb or store energy through some auxiliary compliance mechanisms, such as springs and dampers, so that it can naturally comply with external forces when it is in contact with the environment. The passive compliance control method of robot polishing mainly depends on the end-effectors and polishing tools.

To implement the compliant control during robot assisted polishing, different kinds of end effectors have been designed. The robot force-controlled end-effector should develop in the direction of high precision, multi-degree-of-freedom flexibility, intelligence, and high frequency response[85].Wei et al.[86] proposed a passive end effector based on a constant force mechanism. As

shown in Fig.22, the vibration caused by the eccentric force was avoided by arranging the symmetrical structure, and the guide rail with the slider was used to neutralize the lateral force. The end effector passively adjusted the contact force, and the constant force motion range acted as a buffer to counteract excessive displacement caused by inertia. It suggested that the designed passive constant force end effector could passively exert a constant contact force on the workpiece within a constant motion range.

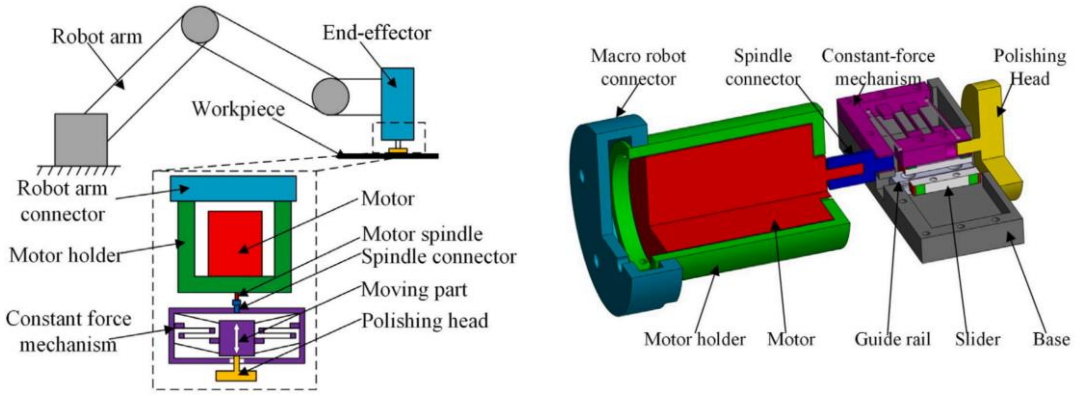

(a) (b)

Fig.22 (a) The schematic diagram and (b) the cross-sectional view of a constant-force end-effector installed on an industrial robot [86].

Du et al. [87] developed an automatic robotic polishing system for titanium alloy curved parts. A flexible end-effector with a force sensor was designed, and a servo motor was used to drive the spindle to avoid the high speed of the traditional pneumatic method, which is easy to cause the problem of resulting in over-polishing. Through the motion control card, the speed of the servo motor can be precisely controlled, and the polishing force can be detected in real time through the sensor. A position-based explicit force control system was established, and an adaptive anti-windup integral separation fuzzy PI controller was used to control the normal contact force to prevent undesired vibration and mechanical collision. Mohammad et al. [88] designed a new novel end-effector, as shown illustrated in Fig.23, which is extended and retracted by a linear hollow voice coil actuator, reducing vibrations that might be caused by inertial effects. Through the integrated force sensor, the polishing force was measured in real time and fed back to the controller. The experimental results showed that the design has less overshoot, less time consuming and less tracking deviation. Mizugaki et al. [89] proposed a novel metal mold polishing robotic system and designed a compliant end effector. The end effector consisted of a pneumatic grinder, spring coils and side guides driven by stepper motors. The tool path was composed of the nominal path of the mould model surface and the offset based on the contact pressure of the end effector elasticity, which can effectively prevent the edge from being over-polished.

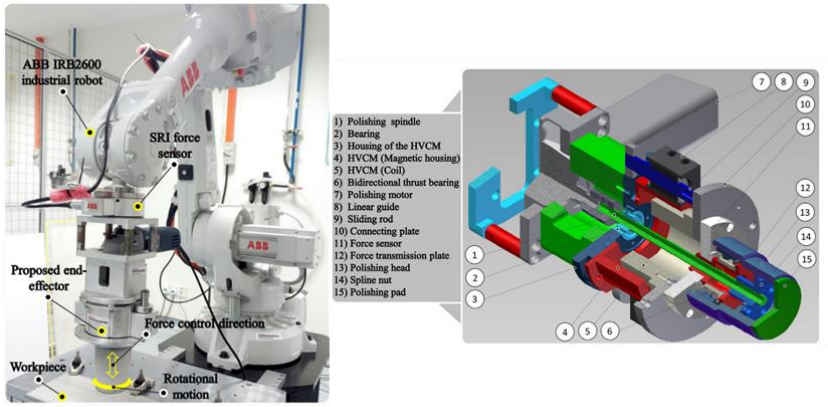

(a) (b)

Fig.23 (a) The photograph of robot polishing system and (b) the schematic diagram of internal structure of end effector [88].

Mohammad et al. [90-92] presented the design of a novel end effector and a method for automated electrochemical mechanical polishing (ECMP) of conductive materials. As shown in Fig.24, the proposed end effector employed three different actions to improve the material removal process in an electrically, chemically, and mechanically coordinated manner. In addition, for this system, a control strategy using neural network and genetic algorithm to optimize polishing parameters was proposed.

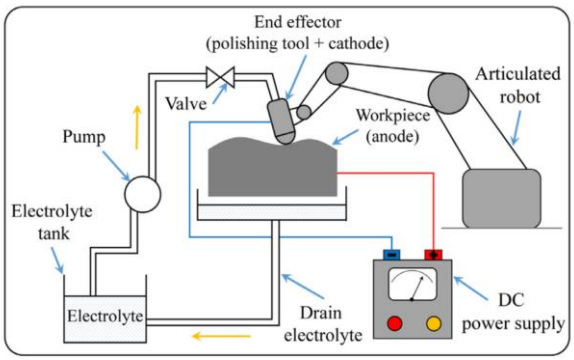

Fig.24 The schematic diagram of robot-based ECMP system [90].

Aiming at the problem that the polishing of thin-walled plates is prone to vibration and seriously affects the surface quality, Chen et al. [93] proposed an intelligent end effector for active contact force control and vibration suppression in robotic polishing. To keep the contact force between the polishing tool and the workpiece at a desired value, a gravity-compensated force controller and two novel eddy current dampers were designed and integrated into smart end effectors to improve system dynamics and dampen vibrations. Wang et al. [94] designed a novel force-controlled end effector and integrated it into the robot, as shown in Fig.25. The experimental results showed that the vibration amplitude of the workpiece is reduced by 75%, and the system can effectively suppress the vibration and improve the grinding stability.

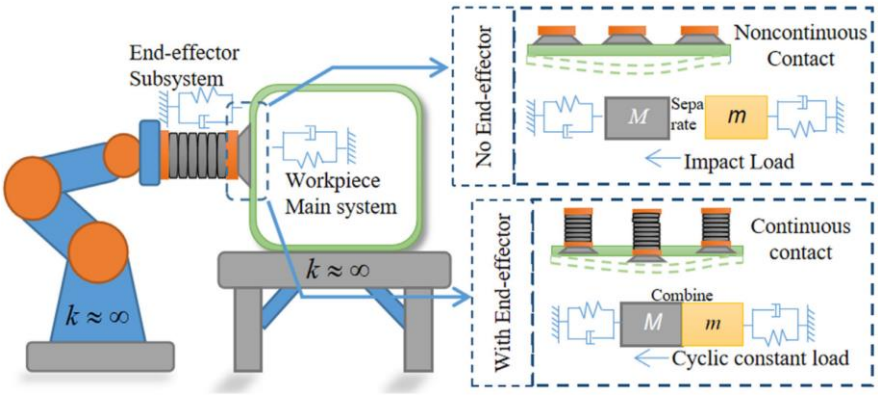

Fig.25 The schematic diagram of grinding robot for thin-walled parts based on force control [94].

Huang et al. [95] established a robotic blade polishing system for turbine blade grinding and polishing, and designed a passive compliant tool as shown in Fig.26. During the polishing process, when the thickness of the blade was large and the removal was insufficient, the contact wheel and spring would be depressed to improve material removal by increasing the polishing force. The sensitivity of the contact force to the brazed layer variation can be adjusted to the required level by changing the spring stiffness and the pre-load. The sudden changes of the machining profile and the vibration generated during the machining process can be greatly attenuated by adjusting the damping coefficient. Ang et al. [84] studied the passive compliance of the robotic arm itself and the end effector. Moreover, Furukawa et al. [96] designed a passively compliant end-effector, which provided a large range of compliant motion that enables the robot to move in a point-to-point manner, simplifying the robot's control algorithm.

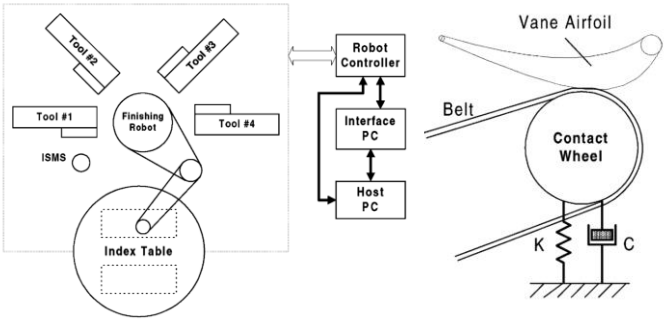

(a) (b)

Fig.26 (a) The schematics of a robotic blade polishing system and (b) the passive compliant polishing principle for blade polishing [95].

Brecher et al. [97] designed an axially flexible polishing tool, which was mainly composed of an annular orbital motor, a spindle motor, a reduction gear train, and an axially flexible compensation component, as shown in Fig.27. The polishing tool was driven by the circular track motor to move in the direction of the circular track after the deceleration of the reduction gear train. The polishing tool was driven by the spindle motor to rotate after passing through the deceleration mechanism and the intermediate transmission parts. Meanwhile, the polishing tool was driven by the axial flexibility compensation component to reciprocate through the cylinder piston rod, to achieve the axial compliance compensation.

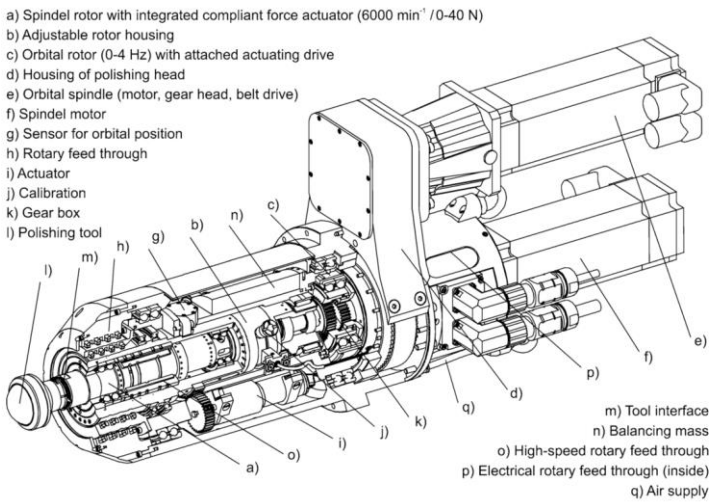

Fig.27 The schematic diagram of internal structure of the axially flexible polishing tool[97].

Wu et al. [98] designed a novel force-controlled wheel polishing tool that combines self-rotation and co-rotation. As shown in Fig.28, this design improved the flexibility of the blade. By optimizing the ratio of the rotation speed to the rotation speed of the end effector, the polishing force fluctuation caused by the robot positioning deviation can be effectively reduced, and a stable symmetrical Gaussian removal function can be obtained. Wahjudi et al. [99] studied a wheel-type polishing tool to achieve control of polishing force by adjusting the z-position through a control system consisting of a load sensor, an interface system, and a computer as a controller.

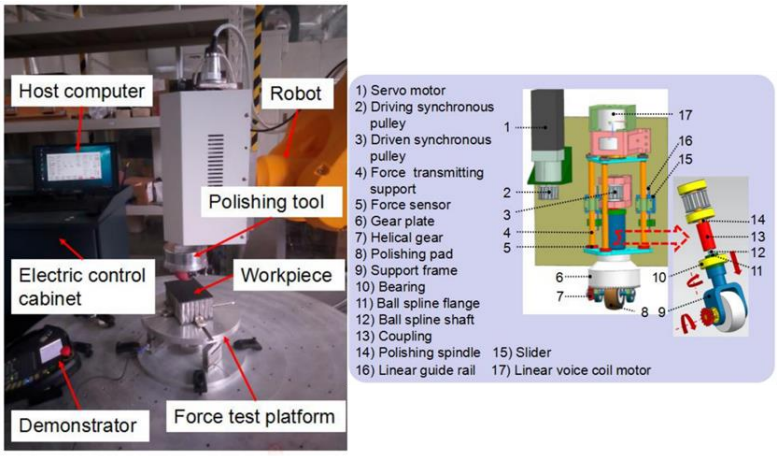

(a) (b)

Fig.28 (a) The photograph of robot-assisted polishing system and (b) the structure of the force-controlled wheel polishing tool [98].

Xu et al. [100] built a robotic abrasive belt polishing system. As shown in Fig.29, a kind of hybrid force control algorithm with Kalman filter information fusion is established. The active-passive hybrid force control method effectively improves the force control accuracy of the robot. Accordingly, both the over-polishing and under-polishing can be suppressed.

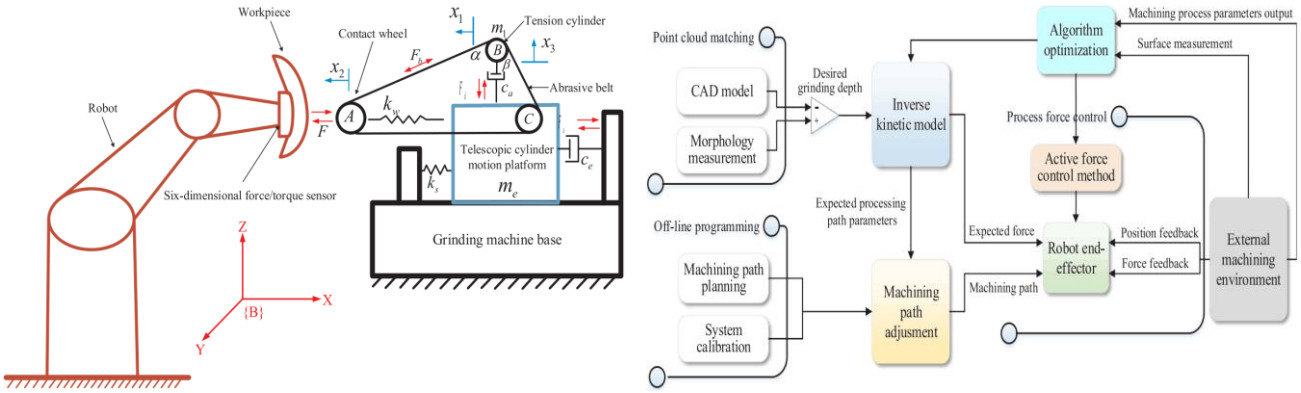

(a) (b)

Fig.29 The photograph of robotic belt polishing system [100].

3.2 Active compliance control

Compared with other methods, and passive flexibility has strong specificity, poor adaptability and larger limitations. Due to the stiffness limitation of the robot itself, it is difficult to achieve high-precision polishing, so it is mostly used in scenes with low precision requirements. The active compliance control can effectively make up for the defects of passive compliance control and further improve the compliance control ability of the system. Active compliance means that based on position control, the robot uses the force feedback information to adopt certain control strategies to actively control the force, which is called active compliance [101,102].This method is currently the mainstream control scheme for robot-assisted high-precision polishing.

Zeng et al. [103] gave a detailed overview of the robot force control algorithms before the twentieth century. It can be inferred that a good force control algorithm is required to achieve high stability and choose the feedback strategy. In fact, a rapid learning ability is also needed to deal with the changes of the robot and the external environment, and stronger robustness is still required to adapt to the disturbance of the external environment. Zhou et al.[104] supposed that the compliant control method can be roughly divided into two categories: direct method and indirect method. The direct method refers to the direct control of force and motion respectively, while the indirect method refers to the control of the dynamic relationship between force and motion to achieve compliant motion. The main control strategies can be divided into the following categories: the force /position hybrid control, impedance control, proportional integral derivative (PID) control, adaptive control, and other control algorithms.

The force /position hybrid control is a direct force control method. As shown in Fig.30, a CAD/CAM-based position/force controller for the control problem of the mold polishing robot was designed by Nagata et al.[2,105]. A force feedback loop was used to control the polishing force consisting of contact friction force and kinetic friction force to achieve stable force control and precise feed control along the curved surface. Ding et al. [106] proposed an adaptive force-position hybrid control method to improve the polishing quality of robotic surfaces. It realized the contact force control of the polishing process without modifying the hardware of the robot, so that the polishing system of different polishing tools had better force tracking performance. Dong et al. [107] proposed a hybrid

position/force control method based on an internal joint torque controller. This method can detect and control the contact force under the condition of strong vibration interference. Accurate force control in actual robotic surface polishing was achieved. The position/force hybrid control frame can well inhibit the occurrence of strong disturbance while maintaining the polishing force control accuracy, which greatly improves the polishing surface quality.

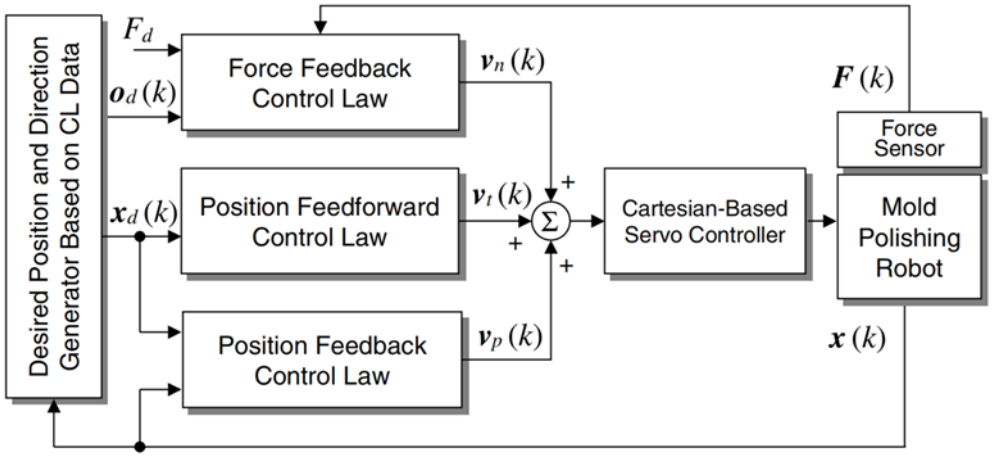

Fig.30 Block diagram of the position/force control system of polishing robot based on CAD/CAM[105].

In terms of sliding model control algorithm, a force-position hybrid control algorithm based on task priority was investigated by Solanes et al.[108]. The polishing force of the robot was controlled by the sliding mode force control method. The position was controlled by a continuous tracking controller. Several chatter-free controllers were tested in the robotic system to verify the effectiveness of the algorithm. Lee et al. [109] developed a five-DOF robot polishing system and proposed a sliding mode control algorithm with velocity compensation, which effectively reduced the robot's tracking error.

Impedance control is an indirect compliant control method that achieves compliant motion by controlling the dynamic relationship between force and motion. Lakshminarayanan et al. [110,111] established a robotic chamfer polishing system as shown in Fig.31 (a), and proposed a Lissajous curve-based model to generate the tool path for chamfering, and proposed a tool path. As shown in Fig.23(b), an iterative learning controller based on impedance control that adapts both position and forces simultaneously in each iteration to regulate the polishing process is proposed. The experimental verification showed that the system has positive polishing effect on the chamfering of titanium, aluminum, and wood. Ochoa et al. [112]proposes an impedance control architecture for human-robot skill transfer of mold polishing tasks. Experimental results showed that the proposed method has good performance in position and direction tracking. Zhou et al.[104] proposed a hybrid control strategy for grinding and polishing robot is based on adaptive impedance control. The experimental results showed that the contact force was stable at 10±3N.

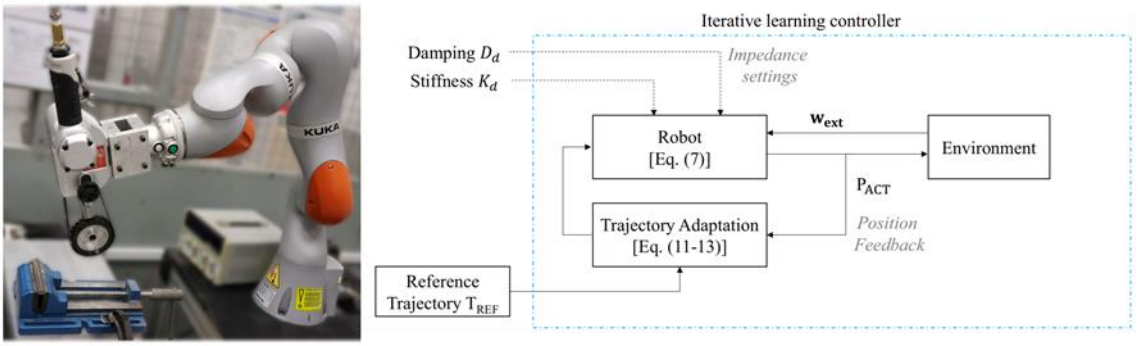

Fig.31 (a) The photograph of Robotic chamfering and polishing system and (b) the iterative learning controller based on impedance control [110,111].

PID control is widely used because of its simplicity and robustness[71,113]. Guo et al. [114] developed a polishing force control system. As shown in Fig.32, the linear stage driven by a stepper motor was employed to prevent force change beyond the travel range of piezo stage which led to the system out of control. Based on the measured force, a PID controller was used to calculate the command voltage to drive the piezoelectric stage. The polishing force was feedback controlled in real-time with a higher force control resolution. Wang et al. [115] proposed a robot-assisted surface machining system based on an active power controller. The PID-plus-feed forward (PIDFF) controller can effectively examine the changes of polishing contact force, apply the required polishing pressure in the normal direction of the workpiece surface, and adjust the contact angle between the hand grinder and the workpiece surface. The research showed that the developed polishing robot system has the ability to polish freeform workpieces. Liao et al. [116] combined pressure sensing and extended sensing to develop a dual-purpose flexible tool for polishing and deburring. The PID controller pre-planned the tool pressure according to the geometry of the workpiece and used the pressure sensor for pressure tracking; the tool extension sensor was used to adapt to the currently required tool length.

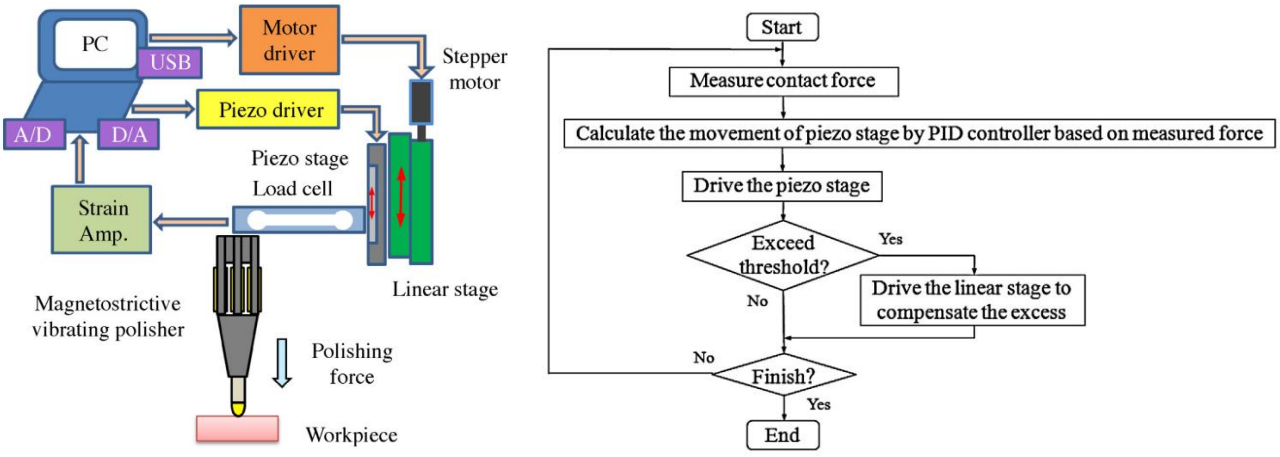

Fig.32 (a) Schematic illustration of the polishing force control system and (b) flow chart of control system program [114].

Many scholars combine adaptive algorithms with other force control algorithms to achieve better control effects. Feng et al. [117] proposed an adaptive fuzzy hybrid control algorithm based on expected contact force. As shown in Fig. 33, Zhan et al. [118] proposed a new and improved hybrid motion/force control method. After introducing a contour-adaptive flexible control strategy, the position and pose errors of the polishing tool were reduced and their interference to the polishing force was suppressed.

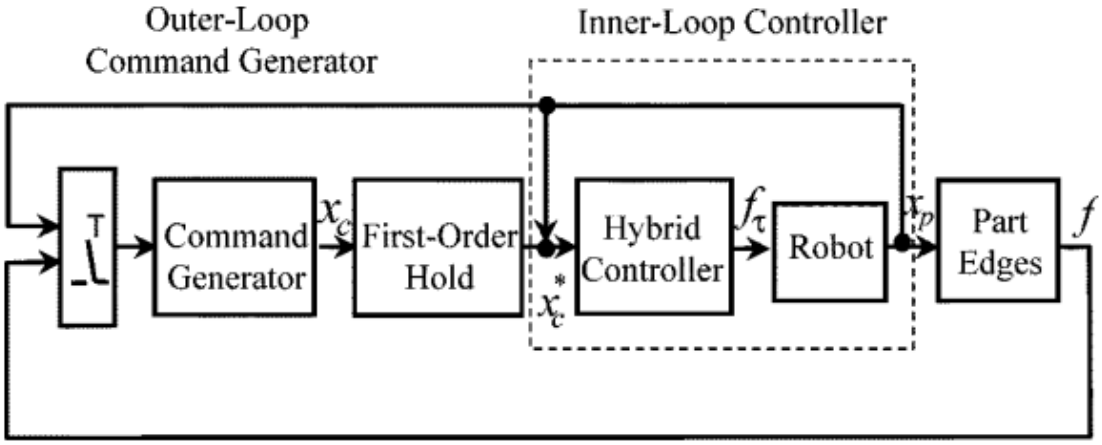

Fig.33 The control architecture of the deburring robot [118].

Minami et al. [119] built a model to describe the motion of a constrained dynamic system of a robot. The constraint force was expressed as a function of state and input, and the robot grinding force was controlled without the use of a force sensor by computing the force instead of the sensor. Thomessen et al. [120] proposed an active power feedback robotic control system for robotic grinding of large hydro turbines. Roswell et al. [121] conducted a detailed study on the contact stress during polishing. The relationship between friction torque and contact stress was discussed in depth for both Hertzian contact and non-Hertzian contact. Tsai et al. [122] developed a robotic mold automatic polishing system and proposed the uniform material removal (UMR) model. It indicated that a free-form surface can be roughly divided into three points: a convex ellipse point, a concave ellipse point and a hyperbolic point. The corresponding contact area was calculated, and the polishing force was controlled according to the effective contact area to achieve uniform removal. Wan et al. [123] elaborated the mechanism of the formation of medium-high spatial frequency error by discrete abrasive particles. It can be confirmed that the rolling wear of particles on the workpiece can reduce the spatial frequency error. In order to reduce the spatial frequency error caused by the asymmetry of particle pressure, an active semi-rigid tool is designed to make the particle pressure symmetrical. Tian et al. [124] detected the polishing force online based on a force sensor, and established a polishing pressure control model to achieve constant force polishing. This method not only removed the workpiece surface material uniformly, but also greatly improved the surface quality. As shown in Fig.34, Jin et al. [125] analyzed the effect of downward depth and inflation pressure on the contact force experimentally, established a contact force control model and constructed a contact force control system. The purpose of the online controllability of mold polishing contact force and uniform surface quality was realized. Shibuya et al. [126] established a robotic mold polishing system. A six-axis force-torque sensor was installed on the robot to adjust the normal force applied on the plane to a target value by changing the height of the hand. The experimental results showed that the system could eliminate EDM marks. A

Pilger die polishing system based on minimum prior information was proposed by Sharma et al. [127]. The symmetry of the mold is used to calculate the local direction of the surface normal, and the polishing force was remained at a constant value of 10 N. The surface roughness of the mold after polishing was reduced to be within the range of 0.2 - 0.4 μm RMS.

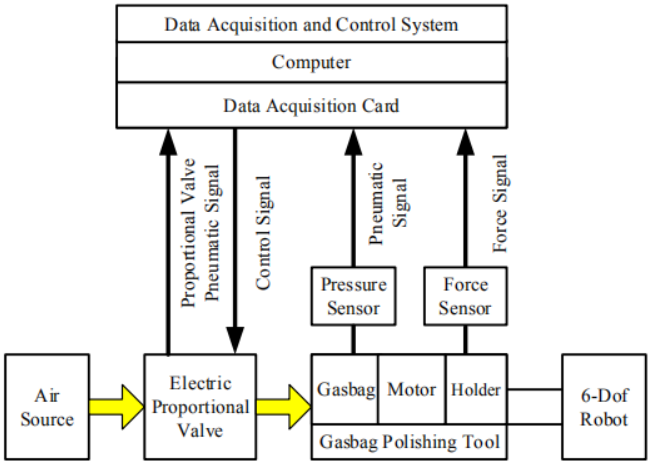

Fig.34 Principle diagram of coupling contact force control system [125].

4. Error analysis and compensation technology of robot-assisted polishing

As mentioned in the introduction section, the relatively limited motion accuracy of a robot system is mainly determined by its structural characteristics. As shown in Fig.35, due to the positioning error of the robot, there is a certain error between the actual position and the theoretical position of the polishing action point, which will reduce the polishing quality. This situation brings new challenges to precision machining. To better improve the motion accuracy of industrial robots and improve the machining accuracy of robot-assisted polishing, it is particularly important to analyze and compensate the errors of industrial robots. This section introduces the research progress of current related work from the perspectives of error analysis of robot kinematics model, robot error compensation, and other types of error analysis and compensation.

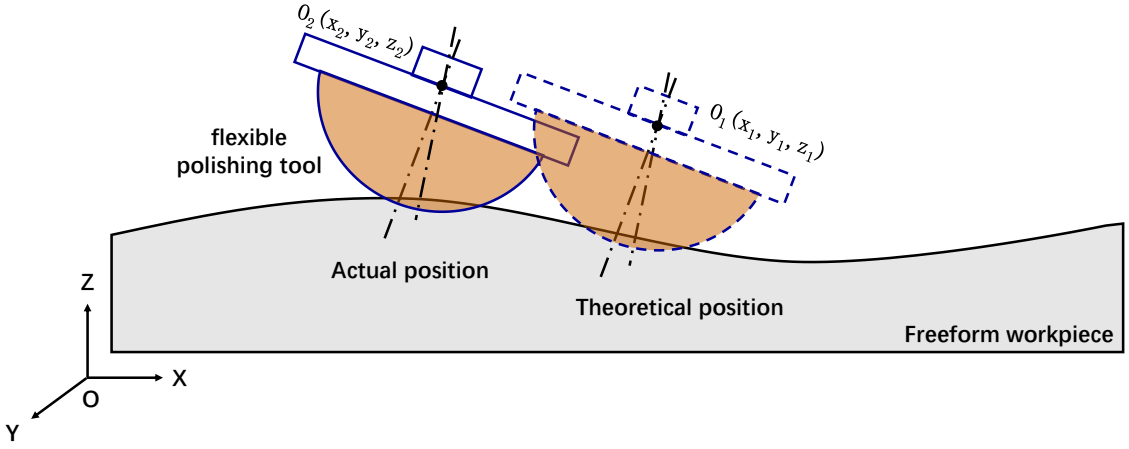

Fig.35 Error of robot-assisted polishing system.

4.1 Error analysis of robot kinematics model

Robot positioning errors are mainly derived from geometric errors and non-geometric errors. Roth et al. [128] divided robot error calibration techniques into three levels: joint level, kinematic level, and non-kinematic level. Robot position errors mostly are originated from geometric errors [129,130]. Robot stiffness and environmental factors are the main sources of non-geometric errors [131,132] and the stiffness of industrial robots is much smaller than that of machine tools [133]. In general, the position repeatability of small robots with lower loads is higher (up to 0.01 mm), and the accuracy of large robots with larger loads is relatively lower.

The positioning accuracy of the robot can be roughly divided into positioning accuracy and position repeatability [134,135]. Positioning accuracy is described as the closeness of the actual position and pose of the robot to the position and pose predicted by its controller; positioning repeatability refers to the accuracy of the robot's endpoints reaching a specific pose (endpoint position and orientation) under repeated instructions from the same joint angle set. Fig.36 shows some typical cases describing the positioning accuracy and position repeatability.

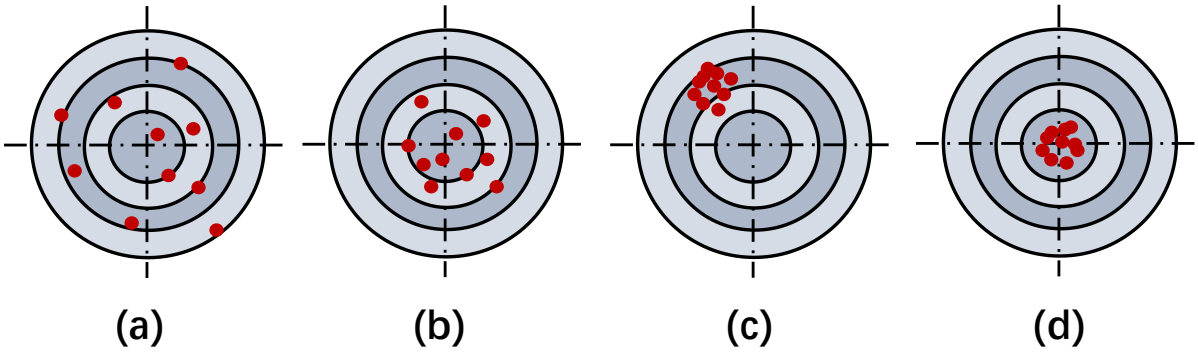

Fig.36 Different scenarios of the combination of positioning accuracy and position repeatability. (a) The positioning accuracy is low, and the position repeatability is low; (b) The positioning accuracy is high, and the position repeatability is low; (c) The positioning accuracy is low, and the position repeatability is high; (d) High positioning accuracy and position repeatability.

The positioning error analysis of the robot mainly includes three steps: kinematic modeling, robot positioning accuracy measurement and parameter identification. Researchers have done a lot of exploration in these aspects owing to the wide application of the industrial robots.

4.1.1 Kinematic modeling

A suitable kinematic error model is required to be established for the error calibration. For instance, Roth et al. [128] pointed out that a complete error model should had three characteristics: completeness (the model has sufficient parameters to express all error factors), continuity (the model is a continuous function of geometric parameters), and minimality (the model has no redundant parameters exist).

Amount of robot modeling methods have been documented to solve the problems of singularity and mutation in modeling. In 1955, Denavit and Hartenberg [136] first proposed a kinematic parameter

model. The DH model contains the four geometric parameters of connecting rod length, connecting rod rotation angle, joint distance, and joint rotation angle to describe the pose relationship between the robot connecting rods, and then realizes the kinematics modeling of industrial robots. Based on this, the mapping relationship between the robot geometric parameter error and the end pose error was established through the differential operation of the matrix. This classical kinematic expression method has been widely used in the research of error modeling and parameter identification of robots. Hayati [137] and Judd [138] proposed a 4-parameter MDH model for rotating joints based on the original DH model, and introduced an additional rotation parameter β for the parallel axis. However, as two adjacent axes are approximately perpendicular, the model seems to be singular. Stone et al. [139] proposed an S-mode, which described the coordinate transformation relationship of adjacent members with 6 parameters and allowed the joint coordinate system to be set arbitrarily. Such method is usually used to solve the problem of parallel axis singularity, but the introduction of additional parameters makes the model redundant.

Okamura et al. [140] applied the product of exponentials (POE) formula to serial robot calibration, and proposed a general error model for serial robot calibration based on the POE formula. The kinematic parameters in the POE formula change with the joint axis and smooth changes. After that, POE formula and local POE formula are applied to robot calibration. He et al. [141] proposed a general error model for tandem robot calibration based on POE formulation. Cho et al. [142] proposed an improved POE-based kinematics model and kinematics calibration method for flexible joint robots. The geometric errors were broadly grouped according to different sensitivities, and established a corresponding recognition model, using a joint correlation error model and multiple recognition spaces to calibrate the six-degree-of-freedom robot, which improved the recognition accuracy of geometric errors[143].

4.1.2 Robot positioning accuracy measurement

Precision calibration is the basis to obtain high accuracy measurement. Under this situation, several different methods have been used to measure the pose data and position data of the robot through equipment such as ball bar, three-coordinate measuring machine, laser tracker and industrial camera. As early as 1993, Goswami et al. [144] proposed a calibration method based on a single ball bar. In 2006, Huang et al. [145] calibrated a five-degree-of-freedom robot using a dual ball bar. As shown in Fig.37(a), Albert et al. [146] used the QC20-W ball bar system to calibrate the positioning accuracy of the robot, and the average positioning error was reduced from 0.873 mm to 0.479 mm. Driels et al. [147] used a coordinate measuring machine to calibrate the PUMA560 robot showed in Fig.37(b). Additionally, Dacheng et al. [148] used the three-coordinate method to calibrate the parallel robot, which effectively reduced the root mean square error of the pose. The theodolite automatic measurement tool requires a lot of time, and the instrument is bulky and unportable. The measurement accuracy largely depends on the operator's level of skill and the quality of the measurement environment [149]. Fraczek et al. [150] proposed a kinematic calibration algorithm using two automatic theodolites, and successfully calibrated the positioning accuracy of 5-DOF and 6-DOF industrial robots respectively, reducing the robot accuracy from 1mm to 0.2mm. In 1991, Leica launched the world's first laser tracker. Other companies including Faro, API, and Hexagon also developed various laser trackers, the maximum permissible errors (MPE) reached below 20 μm. Laser trackers have the

advantages of portability, fast measurement speed, and high measurement accuracy. Laser trackers are widely used in robot precision measurement. As shown in Fig.37(c), Albert et al.[151] used the least squares optimization technique to find the 29 error parameters that best fit the measures acquired with a laser tracker. After calibration, the mean/maximum position errors of ABB IRB 1600 industrial robot are reduced from 0.968 mm/2.158 mm respectively, to 0.364 mm/0.696 mm. Vision based robot calibration has attracted many researchers' interest. Zhang et al. [152]used the local POE formulation to perform kinematic calibration of a UR5 robot through stereo vision. Du et al. [153]proposed an efficient automatic approach to detect the corners from the images of the calibration board. As show in Fig.37(d), camera is rigidly attached to the robot EE to capture the images of the calibration board automatically during the working time.

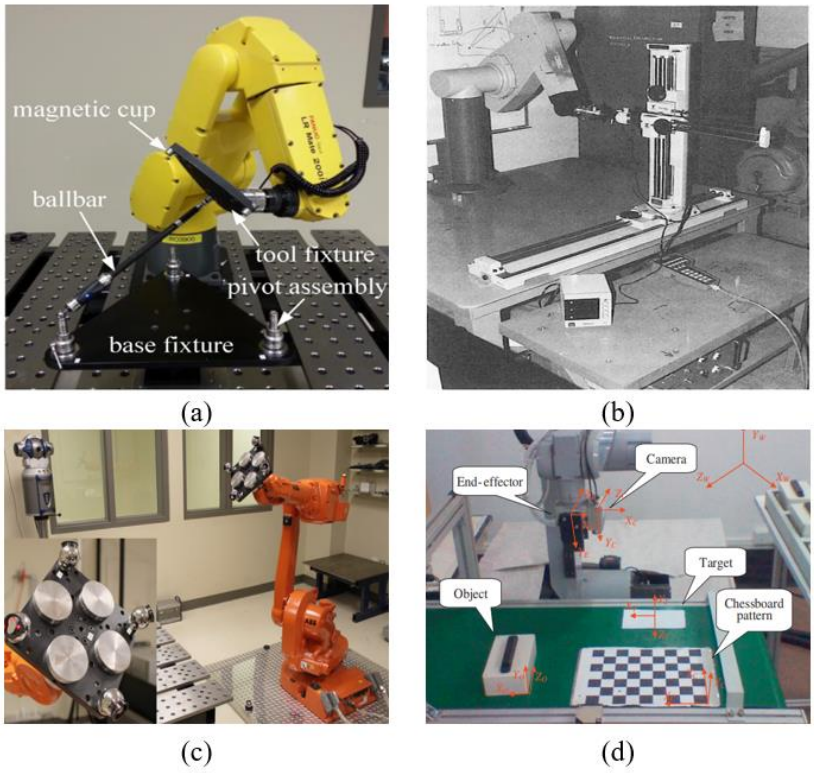

Fig.37(a) Ball bar calibrated QC20-W robot [146] ; (b) CMM calibrated PUMA560 [147];(c) . Faro laser tracker calibrated ABB IRB 1600 robot[151]; (d) Camera calibrated GOOGOL GRB3016 robot[153].

4.1.3 Parameter identification

Parameter identification is a process of identifying the model parameter errors of the robot based on the measured end pose errors, combined with numerical analysis algorithms or optimization methods.

The least-squares algorithm[154] is the most common parameter identification method. The compensation value of each kinematic parameter under the constraint is calculated by algorithm, indicating that the sum of squared errors of the measurement data is the smallest by least-square fitting of redundant data. Noteworthily, the disadvantage of this method is that it can merely improve the accuracy of the area where the reference points involved in the calibration are located, and the accuracy of the measurement points beyond this area has a large deviation. Zhou et al.[155] reported a hybrid

least-squares-GA-based algorithm. As shown in Fig.38, this algorithm can simultaneously identify the defined geometric and non-geometric parameters through a comprehensive error model that includes kinematic and compliance errors.

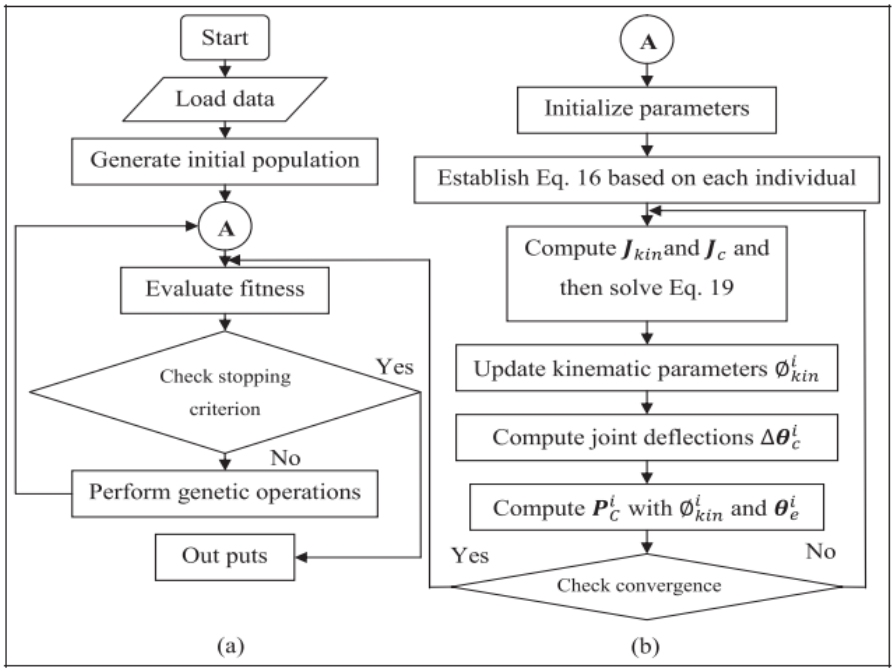

Fig.38 Flowchart of the hybrid least-squares-GA-based algorithm: (a) GA and (b) iterative least-squares algorithm[155].

Martinelli et al. [156] introduced two filtering methods of augmented Kalman filtering and observable filtering to estimate systematic and non-systematic odometry errors, and calibrated mobile robots. Du et al. [157] proposed a robot tool pose estimation method combining particle filter (PF) and Kalman filter (KF). After estimating the pose of the robot, the kinematics recognition is carried out by the extended Kalman filter method. Nguye et al. [158] used the extended Kalman filter (EKF) algorithm to model and identify the geometric parameters of the robot, which effectively solved the problem of correcting the error source of the robot. The Levenberg-Marquardt (LM) method [159] is the most widely used nonlinear least squares algorithm. Numerical solutions for nonlinear minimization (local minima) of numbers were provided. Qi et al. [160] used this algorithm to correct the least squares method in 2017 and solved the error model. The maximum likelihood estimation method (Markov estimation method) was used to identify the dynamic parameters of the KUKA 361 IR robot. Liu et al. [161] used a Genetic Algorithm (GA) with global adaptive probabilistic search capability to identify 24 parameters of a 6DOF robot through simulation, which greatly improved the positioning accuracy of the robot.

4.2 Robot positioning error compensation

Error compensation is the last step in the accuracy calibration of the entire robot. After the parameter error identification, although the error value of each parameter has been identified, the kinematic parameters in the controller cannot be modified, as the robot has been completely packaged. Therefore, it is necessary to convert the calculated kinematic parameter compensation amount to

compensate the joint angle by solving the inverse kinematics solution. Currently, there are two main types of error compensation methods: error compensation based on kinematics model and error compensation based on non-kinematics.

4.2.1 Error compensation based on kinematic model

The error compensation method based on the kinematics model can attribute the error factors affecting the positioning accuracy of the robot to the link parameter error or the joint angle error. This method models the kinematic error, calculates the error of the theoretical model parameters, and corrects the error of each parameter to the kinematic model.

The joint space compensation method is directly corrected in the joint space according to the calibration result, and the joint value that can reach the target pose is recalculated. Devlieg and Szallay [162,163] used the joint space compensation method to compensate the error of the industrial robot. To further improve the positioning accuracy of the robot, an additional secondary encoder was used to perform high-precision closed-loop control of the rotation angle of each axis. The methods of robot error compensation are divided into two types. The first type is the methods based on the correction of the joint displacements of the desired position and orientation based on the nominal inverse kinematics, and the second type is based on the redefinition of the desired position and orientation before the nominal inverse kinematics. The results showed that the compensation effects of the these two types of methods are equivalent when the variations of parameters are nearly neglected, while the second method does not need to calculate the inverse of the Jacobian matrix and can be used for the odd-shaped robot.

The positioning error of the robot is regarded as a small displacement in the differential error compensation method, and the differential transformation concept was established in the robot error model. Small deviations between the nominal and actual geometric parameters can be calculated and compensated for the nominal parameters of the controller. Veitscheggr et al. [164] used an iterative loop method to calculate the error of each joint of the robot, and used the differential error compensation method and the Newton-Raphson (N-R) compensation method to compensate the error of the robot. Zhong et al. [165] successfully applied artificial neural networks to the approach calibration of robots. The actual pose of the robot and the corresponding joint angle errors were used as the input and output of the feedforward neural network to train the network. Takanashi et al. [166] proposed an improved method for positioning accuracy based on artificial neural network, which automatically recognizes the robot model error through the back-error propagation method. Zeng et al. [167] proposed an error compensation method for error similarity analysis. As shown in Fig.39, by analyzing the error model established by the robot kinematic parameters, the position error similarity is proposed. The position error of the robot TCP was calculated by the ordinary kriging method, and the error compensation was realized by modifying the position coordinates in the robot control command. The experimental results showed that the maximum position error of the robot TCP was reduced by 75.36% from 1.2912 mm to 0.3182 mm. Wei et al. [168] proposed a method for selecting sampling points within a uniform grid based on the error-similar error compensation method. The influence of sampling point position on error compensation was analyzed by numerical simulation, and the grid step of sampling point was optimized by statistical analysis method. The laser tracker was used to compensate the error of the KUKA robot, causing the errors in the X, Y, and Z directions of the robot reduced from 0.193mm,

0.150mm, and 0.252mm to 0.061mm, 0.101mm, and 0.084mm, respectively.

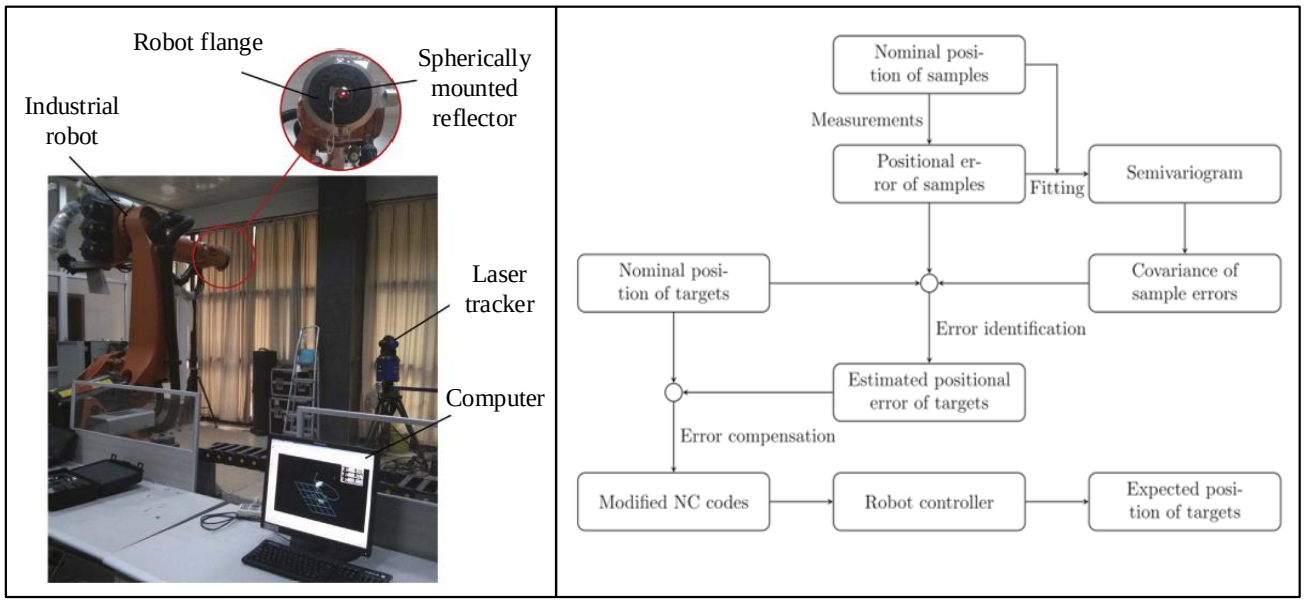

(a) (b)

Fig.39(a) Experimental setup and (b) flowchart of the error identification and compensation method with error similarity[167].

Zhao et al. [169] gave the definition of contour error for 6DOF robot machining tasks. Based on the Fibonacci search and spherical detailed interpolation algorithm, a local iterative robot contour error estimation algorithm is proposed, and contour error compensation is performed for the six-degree-of-freedom robot. Ma et al. [170] proposed a new method for robot calibration and compensation. Using position data measured by a laser tracker, the maximum likelihood to identify error model parameters was obtained. The updated joint commands are determined with a Jacobian-based search method to compensate for the kinematic errors of the robot. Luo et al. [171] put forward a differential evolution hybrid algorithm, and used the LM algorithm to realize the pre-identification of the robot kinematic parameter deviation. The suboptimal value of these parameter deviations is defined as the central value of each component of the initial individual, and the differential evolution algorithm is used to complete the accurate identification. The positioning error of the robot is reduced from 0.994mm to 0.262 mm by the laser tracker. Huang et al. [172,173] performed kinematic calibration of the six-DOF hybrid polishing robot shown in Fig.40. The explicit error model of the hybrid robot was established according to the spiral theory, so as to the linearization error compensator. After calibration, the absolute positioning error of the hybrid polishing robot reached 0.07mm, and the repeated positioning error was only 0.016mm.

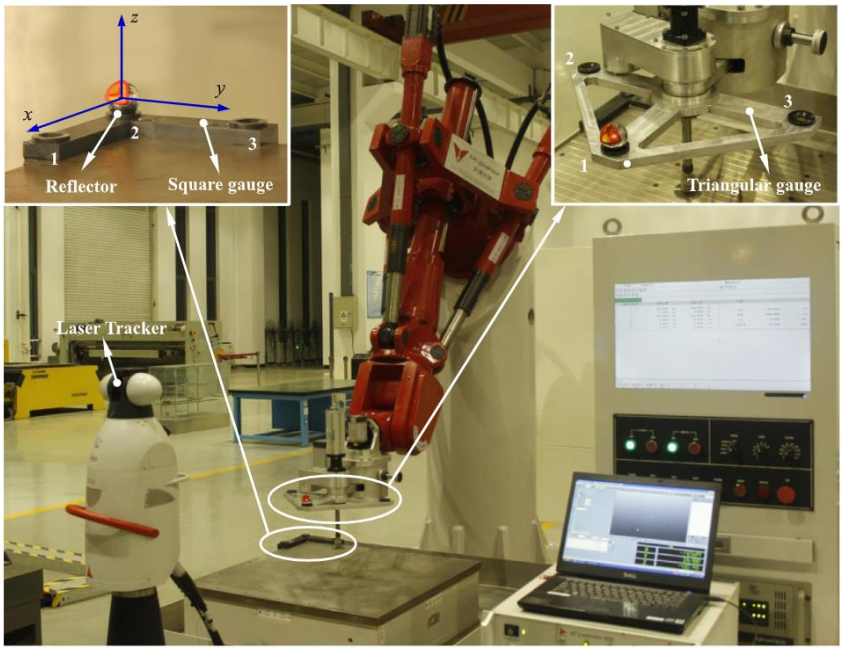

Fig.40 The photograph of six degrees of freedom hybrid polishing robot [172].

4.2.2 Non-kinematic error compensation

Non-kinematic error compensation not only needs to consider the geometric parameter errors of the robot, but also needs to consider errors such as structural deformation errors and dynamic parameter errors.

Joubair et al. [174] considered the influence of kinematic parameters, stiffness errors, world and tool coordinate system parameters on robot accuracy, and proposed a non-kinematic calibration method based on plane constraints. Error compensation was performed on the FANUC robot, and the maximum plane error was decreased from 3.740 mm to 0.083 mm. Jiang et al. [175] proposed an artificial neural network optimized based on differential evolution algorithm. Iteratively updates the structure and parameters of the network through differential evolution, which improves the accuracy and efficiency of the network. Then, the trained network was used to compensate the absolute positioning error caused by motion error and non-motion error. The average positioning error of the robot was reduced from 0.8497 mm to 0.0490 mm.

Combining geometric error, position-dependent compliance error, and time-varying thermal error, a comprehensive error model was established by Gong et al. [132]. These errors were inversely calibrated using a laser tracker, and an empirical thermal error model was established using the orthogonal regression method. This method correlated the thermal error of the robot parameters with the corresponding temperature fields. These models can be applied on the controller to compensate for quasi-static thermal errors due to the presence of internal and external heat sources. The average positioning error of industrial robots was reduced from 1.2 mm to 0.11 mm. As shown in Fig.41, Chen et al. [176] established a rigid-flexible coupling error model, which not only considered kinematic errors, but also compliance errors (the effects of external loads and the self-gravity of the connecting rod).The laser tracker was used to compensate the error of the Staubli RX160L robot, and the average positioning error was significantly reduced from 3.72 mm to 0.23 mm.

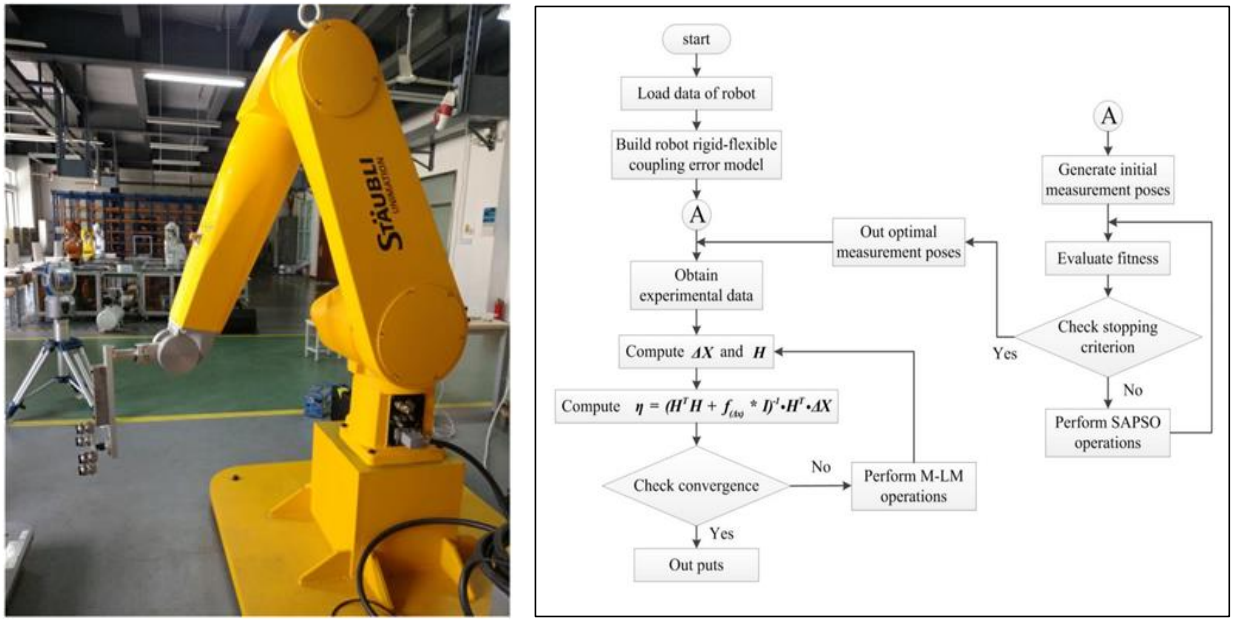

(a) (b)

Fig.41 (a) Experimental platform and (b) flowchart of the optimization approach for robot calibration [176].

4.3 Other error analysis and compensation techniques

4.3.1 Vibration control

Due to the low stiffness and coupled structure of industrial robots, regenerative flutter and mode-coupled flutter occur under various conditions. This phenomenon will seriously affect the surface quality of optical components and blisk[177,178]. Moradi et al. classified vibrations generated during machining into two categories: forced vibrations and self-excited vibrations [179,180]. Quintana et al. [181] discussed that self-excited vibrations (chatter) extract and generate energy from the interaction between the tool and the workpiece during machining, which could have severe effects on the system. Generally, the methods of robot vibration control can be divided into two categories: passive control and active control.

Passive control is mainly used to improve the structural stiffness and damping coefficient of the robot by adding damping, the design of the robot's vibration-absorbing structure, and the using of sensitive materials, so as to reduce the elastic deformation of the flexible system and suppress the residual vibration of the system. Increasing the structural damping can effectively improve the dynamic performance of the flexible joint manipulator. The viscoelastic material is adhered to the flexible mechanism to form a damping layer. With the vibration of the mechanical structure, the viscoelastic damping layer generates alternating stress and strain of tension and compression, thereby consuming mechanical vibration energy and achieving the purpose of vibration reduction. Ganesan et al. [182] studied the effects of the thickness of the viscous damping layer and the thickness of the magnetic mass damping layer on the natural frequency and vibrational energy dissipation rate of the beam. To suppress the vibration of the flexible system, the weight, stiffness, and damping parameters of the system structure are optimized to change the natural frequency and damping ratio of the system.

Moritat et al. [183] designed a vibration-damping structure for a macro-micro arm. Actuators and sensors using sensitive materials as robot joints can feedback vibration signals in real time. Ge et al. [184] studied using shape memory alloys (SMAS) to suppress vibrations of flexible robots.

Active control is to design the corresponding control algorithm according to the dynamic characteristics of the robot. To suppress the joint error of the robot or compensate for the influence of flexibility, reduce the dynamic response of the flexibility, and then achieve the purpose of suppressing vibration [185]. Compared with passive control, active control is more flexible and adaptable. Active control includes feedforward control methods and feedback control methods. The vibration can be largely eliminated / weakened by the feedforward vibration control method while the flexible structure completes the task by adjusting the control command. Feedforward control methods mainly include input shaping method, S-curve method, and trajectory planning. Qiu et al. [186]conducted experimental research on vibration control based on a feedforward controller with input shaping technology and a generalized minimum variance self-correcting control algorithm. Zou et al. [187] proposed an asymmetric S-curve profile method with perturbation in order to reduce the residual vibration under high-precision high-speed motion. The curve interpolation can improve the machining performance, control the acceleration and acceleration well, and eliminate the machining impact caused by the unsatisfactory line[188].Feedback control includes PD (PID) control, sliding mode variable structure control, robust control, adaptive control and so on. Traditional PD or PID control does not need to consider the dynamic characteristics of the robot joint coupling, and only needs to adjust the three parameters of proportional, integral, and differential to achieve effective control of the robot. Ho et al. [189] proposed a H∞PID control synthesis method to design PID controllers to guarantee robust performance under uncertainty. Sliding mode variable structure control has good robustness and rapidity and has been well applied in the control of flexible arms. It is combined with other control algorithms to achieve better vibration control effect. Lochan et al. [190] adopted sliding mode control for tip trajectory tracking control of the master robot. A second order PID terminal sliding mode controller was proposed for synchronization between a controlled master robot and the slave robot. Many advanced control algorithms have been used to solve vibration control problems [191,192], including robust control algorithms and adaptive control algorithms, as well as combinations with other control algorithms. Dubay et al. [193] proposed a control method using the combination of a finite element model and a model predictive controller to suppress vibration at the end of a single-link flexible arm.

4.3.2 Gravity compensation

The robot force control system has high requirements on the precision of the contact force to meet the actual demand. To obtain accurate contact force information, the sensor error should be compensated. In the general working environment, the six-dimensional force sensor is in a static state. The force/torque data recorded by the sensor consists of three parts: the system error of the sensor itself, the gravity of the load, and the contact force of the external environment on the load. In order to meet the requirements of the robot force control system, the influence of the self-system error and the load gravity on the perception force should be eliminated. Therefore, it is necessary to perform gravity compensation on the robot.There are two main methods of gravity compensation: one is to use the compensation made by industrial robot manufacturers using their own offline programming software.

For example, the features of the weight, center of gravity and moment of inertia of the workpiece were added into the ABB's offline programming software, the gravity is compensated; the other one is to use external hardware or algorithm to compensate for the gravity.

Arakelian et al. [194] reviewed the application of gravity compensation in robotics. The balancing solutions are classified into three main categories according to the nature of the compensating force: balancing force, spring force or active force developed by auxiliary actuators. Chen et al. [93] proposed an intelligent end effector for active contact force control and vibration suppression in robotic polishing. To keep the contact force between the polishing tool and the workpiece at a desired value, an intelligent end effector with a gravity-compensated force controller and two eddy current dampers were designed. As shown in Fig.42, the contact force and the relative angle between the global coordinate system and the force sensor axis are measured by force sensor. Gravity compensation with tilt sensors improved system dynamics and dampen vibrations. The experimental results showed that the designed smart end effector can reduce the contact force variation from 8 N to below 1 N, and significantly suppresses the spindle vibration.

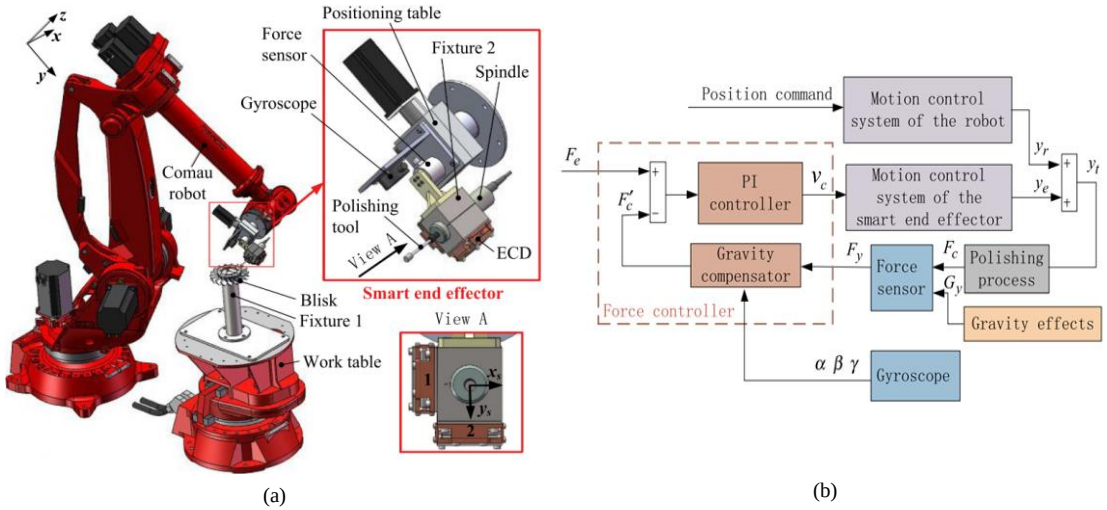

Fig.42 (a) Experimental platform and (b)Block diagram of the active force control system [93].

Ding et al. [106] proposed an adaptive force-position hybrid control method to improve the polishing quality of robotic surfaces. The contact force control of the polishing process could be produced without modifying the hardware of the robot, and performed gravity compensation for the robot, so that the polishing system of different polishing tools had superior force tracking performance. Tian et al. [124,195] proposed a generation algorithm for polishing tool position and pose based on force-position-pose decoupling control for the constant force control problem during polishing. The gravity compensation algorithm of the polishing tool was proposed to eliminate the gravity interference in the machining process. This method greatly improved the surface quality of the robot surface automatic polishing. Zhang et al. [196] proposed a passive/active hybrid control scheme for industrial robots. A six-axis force/torque sensor was used as the main power device, and the tool was gravity compensated at the same time. Gao et al. [197] performed real-time control of the polishing force and proposed a gravity compensation algorithm to keep the polishing force relatively constant.

4.3.3 Robot stiffness optimization

The multi-joint series structure of the robot makes its stiffness lower than that of a machine tool. When the end load of the robot is beyond a critical value, it results in the occurrence of deform and affecting the machining accuracy, so the stiffness of the robot is needed to be optimized.

Salisubury et al. [198] established a robot stiffness model based on the mapping relationship between the end stiffness matrix and the joint stiffness. Chen et al. [199] optimized this model and proposed the conservative congruence transformation (CCT) stiffness model. Alici et al. [200] proposed a modified stiffness model which takes both the stiffness of the joints and the stiffness of the robot under external forces into account. The current robot stiffness modeling methods can be classified into three categories: finite element analysis method, matrix structural analysis method (SMA) and virtual joint method (VJM). The finite element analysis method has high precision, but the calculation amount is large. SMA can reduce computation, but it cannot provide the physical relationships required for parametric stiffness analysis. Based on the traditional stiffness model, the VJM method describes the deformation of links and joints by adding virtual joints. Klimchik et al. [201] adopted the virtual joint method (VJM) to establish the stiffness model of the robot, with a 6 × 6 stiffness matrix as each compliant link and a scalar coefficient as the joint/transmission coefficient, considering all mechanical elements (such as rods, driven joints and mechanical transmissions).

Dumas et al.[202] determined the optimal robot configuration based on the kinematic matrix. The robot stiffness model was established by the Cartesian stiffness matrix and the complementary stiffness matrix to realize the rapid identification of the robot stiffness value. Rui et al.[203] used the improved genetic algorithm to replace the least square method for stiffness identification, which avoided the influence of the initial value on the calculation result and improved the compensation effect of stiffness error. The average distance error and the maximum distance error of the industrial robot after stiffness error compensation were 0.2485 mm and 0.3332 mm, respectively. Compared with the distance positioning error before stiffness error compensation, the robot positioning accuracy was improved by 33.7%. Abele et al. [204] proposed a method for calculating stiffness in Cartesian coordinates based on polar stiffness and Jacobian matrix. Christianl et al. [205] obtained data such as joint position and velocity through the robot controller, and measured the force and torque of the end effector to determine the robot stiffness for parameter identification. Based on the translational compliance submatrix (TCSM), Guo et al. [206] used the stiffness deformation ellipsoid to evaluate the stiffness performance of the robot, which can be used to calculate the stiffness of the robot in different coordinate systems.

5. Summary and outlook

From the perspective of practical industrial application, robot-assisted polishing technology can not only meet the requirements of high precision and high quality, but also provide high work efficiency and flexible working range. Hence, it has been widely used in the polishing of components in different fields. In the past decades, remarkable advances have been achieved in the areas of design and optimization of various polishing tools, constant polishing force control methods, positioning error modeling, and compensation technique. The future research and development directions towards

further improving the polishing performance of robot-assisted polishing are summarized as follows:

1) Improvement of robot positioning accuracy. Compared with the conventional machines, industrial robots have flexible working ranges, and the processing of large workpieces exhibits greater advantages. However, the positioning accuracy and position repeatability of the robot-assisted polishing technique are still insufficient. This is limiting its potential application for ultra-precision polishing. Furthermore, due to robot load and stiffness constraints, the feed rates of the polishing tool, as well as the size and weight of the polishing tool should be kept small, this largely limits the material removal rate and processing efficiency. Therefore, it is necessary to further improve the accuracy of the robot from the mechanics and control aspects. Affected by the serial mechanical structure of the robot, the stiffness is poor, and the mechanical accuracy is difficult to improve, so it is necessary to focus on error compensation strategies. Although some error compensation methods have been successfully developed, it is still difficult to meet the ever-increasing needs required for the polishing ultra-precision components. Therefore, the research on more advanced robot positioning error compensation methods will still be an active research area in the future, the combination of machine learning would be competitive solution for this problem.

2) Stable control of polishing force. Polishing force is closely related to the robot motion error, which significantly affects the polishing capability. Adaptive stable control of polishing force is crucial, which can restrain the influence of robot motion error. With the rapid development of machine learning, the stability and anti-interference ability of force control algorithms will be further developed. The flexibility of processing and the quality of the processed surface can be improved by the combination of machine vision, constant force control, and intelligent algorithms. In addition, although various constant force control algorithms have been proposed, the response time is still quite long, resulting in a large compensation error. Therefore, it is still necessary to further improve the sensitivity of the polishing force compensation system to implement fast response or even close to 'real-time' compensation.

3) Optimized design of polishing tools. With the gradual development of industrial robots, they are massively integrated in numerous polishing methods that have been conventionally performed by CNC machines. The application of robot-based polishing tool is still increasing, leading to the requirement of optimized designs of these tools to meet the polishing requirements of high precision and stability.

4) Multi-robot collaborative polishing. Robot-assisted polishing has been applied to the polishing of large-aperture optics such as telescopes. Nonetheless, due to the large size of the mirror, the processing efficiency is still limited even if large polishing tools are used. Therefore, multi-robot collaborative polishing can be considered in the future to improve the throughput of a polishing system. In addition, multiple polishing tools with different correction capabilities can be used to correct a wide range of spatial frequencies.

Acknowledgments

This work was supported by the Natural Science Foundation of Fujian Province, China (2022J011245).; the research office of the Hong Kong Polytechnic University (Project code: BBXL, BD9B); Accelerator and Detector Research Program (FWP# PS032); Office of Science of the United States (DE-SC0012704); Brookhaven National Laboratory (BNL LDRD 17-016).

References

[1] Cheung, Kong, Ho, To. Modelling and simulation of structure surface generation using computer controlled ultra-precision polishing. Precision Engineering (2011)35, 574-590.

[2] Nagata, Kusumoto, Fujimoto, Watanabe. Robotic sanding system for new designed furniture with free-formed surface. Robotics and Computer Integrated Manufacturing (2006)23.

[3] Pitschke, Schinhaerl, Rascher, Sperber, Smith, Stamp, Smith. Simulation of a complex optical polishing process using a neural network. Robotics and Computer Integrated Manufacturing (2006)24.

[4] Walker, Freeman, McCavana, Morton, Riley, Simms, Brooks, Kim, King. Zeeko/UCL process for polishing large lenses and prisms. Proceedings of SPIE - The International Society for Optical Engineering (2002)4411, 106-111.

[5] Walker, Beaucamp, Doubrovski, Dunn, Evans, Freeman, Kelchner, McCavana, Morton, Riley, et al. Automated optical fabrication: first results from the new Precessions 1.2m CNC polishing machine. In Proceedings of Proceedings of SPIE - The International Society for Optical Engineering, 2006.

[6] Schindler, Hänsel, Frost, Fechner, Nickel, Thomas, Neumann, Hirsch. Ion beam finishing technology for high precision optics production. In Proceedings of Optical Fabrication & Testing.

[7] Shorey, Kordonski, Tricard. Magnetorheological finishing of large and lightweight optics. Proceedings of SPIE - The International Society for Optical Engineering (2004).

[8] Jourdain, Castelli, D, Sommer, Shore. Reactive atom plasma (RAP) figuring machine for meter class optical surfaces. Production Engineering (2013)7, 665-673.

[9] Ferraguti, Pini, Gale, Messmer, Storchi, Leali, Fantuzzi. Augmented reality based approach for on-line quality assessment of polished surfaces. Robotics and Computer Integrated Manufacturing (2019)59.

[10] Wang, Yu, Xu. Coordinate transformation of an industrial robot and its application in deterministic optical polishing. Optical Engineering (2014)53.

[11] Lin. Path Generation for Robot Polishing System Based on Cutter Location Data. Advanced Materials Research (2014)902, 250-253.

[12] Li, Wang. Path Planning for Industrial Robots in Free-Form Surface Polishing. In Proceedings of 2019 5th International Conference on Control, Automation and Robotics (ICCAR).

[13] Lu, Zhang, Fuh, Han, Wang. Time-optimal tool motion planning with tool-tip kinematic constraints for robotic machining of sculptured surfaces. Robotics and Computer-Integrated Manufacturing (2020)65.

[14] Kharidege, Du, Zhang. A practical approach for automated polishing system of free-form surface path generation based on industrial arm robot. International Journal of Advanced Manufacturing Technology (2017).

[15] Wan, Zhang, Xu, Wang, Jiang. Region-adaptive path planning for precision optical polishing with industrial robots. Optics Express (2018).

[16] Cao, Zhou, Jiang, Hon, Yi, Dong. An integrated processing energy modeling and optimization of automated robotic polishing system. Robotics and Computer-Integrated Manufacturing (2020)65.

[17] Lv, Peng, Qu, Zhu. An adaptive trajectory planning algorithm for robotic belt grinding of blade leading and trailing edges based on material removal profile model. Robotics and Computer-Integrated Manufacturing (2020)66.

[18] Beatriz, Marta, Roberto, Eva. Analysis of Force Signals for the Estimation of Surface Roughness during Robot-Assisted Polishing. Materials (2018)11, 1438.

[19] Segreto, Karam, Teti, Ramsing. Cognitive Decision Making in Multiple Sensor Monitoring of Robot Assisted Polishing. Procedia CIRP (2015)33, 333-338.

[20] Segreto, Karam, Teti. Signal processing and pattern recognition for surface roughness assessment in multiple sensor monitoring of robot-assisted polishing. The International Journal of Advanced Manufacturing Technology (2016).

[21] Agustina, Marín, Roberto, Eva. Surface Roughness Evaluation Based on Acoustic Emission Signals in Robot Assisted Polishing. Sensors (2014)14, 21514-21522.

[22] Pilný, Bissacco. Development of on the machine process monitoring and control strategy in Robot Assisted Polishing. CIRP Annals - Manufacturing Technology (2015)64, 313-316.

[23] Segreto, Teti. Machine learning for in-process end-point detection in robot-assisted polishing using multiple sensor monitoring. The International Journal of Advanced Manufacturing Technology (2019)103.

[24] Yu, Zhang, Sun, Zhang, Zheng, Wang. Review of Computer Controlled Optical Surface Molding Technology. Optical Technique (1998), 7-9+6.

[25] Jones. Computer-controlled grinding of optical surfaces. Appl Opt (1982)21, 874-877.

[26] Walker, Dunn, Yu, Bibby, Zheng, Wu, Li, Lu. The role of robotics in computer controlled polishing of large and small optics. SPIE Optical Engineering + Applications (2015).

[27] Walker, Yu, Gray, Rees, Bibby, Wu, Zheng. Process Automation in Computer Controlled Polishing. Advanced Materials Research (2016)4231.

[28] Walker, Yu, Gray, Rees, Bibby, wu, Zheng. Process Automation in Computer Controlled Polishing. Advanced Materials Research (2016)1136, 684-689.

[29] HaiTao, YongJian, ZhiGe, LiChao, HongShen, Kai. Freeform surface grinding and polishing by CCOS based on industrial robot. Institute of Optics and Electronics (China);Univ. Bremen (Germany);National Univ. of Defense Technology (China) (2016)9683.

[30] Lin, Jiang, Cao, Huang. Development and theoretical analysis of novel center-inlet computer-controlled polishing process for high-efficiency polishing of optical surfaces. Robotics and Computer-Integrated Manufacturing (2019)59, 1-12.

[31] Liu, Yan, Zhao, Wu, Zhou. Fabrication of SiC Off-axis Aspheric Mirror by Using Robot Polishing. EPJ Web of Conferences (2019)215.

[32] Yu, Kong, Zhang, Xu, Wang. An improved material removal model for robot polishing based on neural networks. Infrared and Laser Engineering (2019).

[33] Cao, Cheung, Zhao. A theoretical and experimental investigation of material removal characteristics and surface generation in bonnet polishing. Wear (2016)360-361, 137-146.

[34] Binghama, Walker, Kim, Brooksa, Freemanb, D.Rile. A novel automated process for aspheric surfaces. Proceedings of SPIE - The International Society for Optical Engineering (2000)4093, 445-450.

[35] Walker, Atad-Ettedgui, D'Odorico, Beaucamp, Bingham, Brooks, Freeman, Kim, King, McCavana, et al. The 'Precessions' tooling for polishing and figuring flat, spherical and aspheric surfaces. Opt Express (2003)11, 958-964.

[36] Kong, Cao, ho. *Bonnet Polishing of Microstructured Surface*; Micro and Nano Fabrication Technology: (2018)Vol. Micro/Nano Technologies, vol 1.pp1-50, Springer, Singapore.

[37] Li, Walker, Yu, Sayle, Messelink. Edge control in CNC polishing, paper 2: simulation and validation of tool influence functions on edges. Opt Express (2013)21, 370-381.

[38] Li, Walker, YU, Zhang. Modeling and validation of polishing tool influence functions for manufacturing

segments for an extremely large telescope. Appl Opt (2013)52, 5781-5787.
[39] Dunn, Walker. Pseudo-random tool paths for CNC sub-aperture polishing and other applications. Opt Express (2008)16, 18942-18949.
[40] Walker, Beaucamp, Dunn, Evans, Freeman, Morton, Wei, Yu. Active control of edges and global microstructure on segmented mirrors. OpTIC Technium (United Kingdom);Zeeko Ltd. (United Kingdom);Zeeko Technologies LLC (United States) (2008)7018.
[41] Walker, Baldwin, Evans, Freeman, Hamidi, Shore, Tonnellier, Wei, Williams, Yu. A quantitative comparison of three grolishing techniques for the Precessions process. Proceedings of SPIE - The International Society for Optical Engineering (2007)6671, 66711H-66711H-66719.
[42] Wang, Wang, Yang, Sun, Peng, Guo, Xu. Modeling of the static tool influence function of bonnet polishing based on FEA. The International Journal of Advanced Manufacturing Technology (2014)74, 341-349.
[43] Pan, Zhong, Chen, Wang, Fan, Zhang, Wei. Modification of tool influence function of bonnet polishing based on interfacial friction coefficient. International Journal of Machine Tools and Manufacture (2018)124, 43-52.
[44] Zhong, Wang, Chen, Wang. Time-varying tool influence function model of bonnet polishing for aspheric surfaces. Applied Optics (2019)58.
[45] Cao, Cheung. Multi-scale modeling and simulation of material removal characteristics in computer-controlled bonnet polishing. International Journal of Mechanical Sciences (2016)106, 147-156.
[46] Zhong, Huang, Chen, Wang, Pan, Wen. Impact of pad conditioning on the bonnet polishing process. The International Journal of Advanced Manufacturing Technology (2018)98, 539-549.
[47] Wang, Yang, Wang, Yang, Sun, Zhong, Pan, Yang, Guo, Xu. Highly efficient deterministic polishing using a semirigid bonnet. Optical Engineering (2014)53.
[48] Wang, Wang, Wang, Ke, Zhong, Guo, Xu. Improved semirigid bonnet tool for high-efficiency polishing on large aspheric optics. The International Journal of Advanced Manufacturing Technology (2017)88.
[49] Pan, Zhao, Wang, Jo, Gao, Chen, Fan. Research on an evaluation model for the working stiffness of a robot-assisted bonnet polishing system. Journal of Manufacturing Processes (2021)65.
[50] Zhong, Xu, Wang, Deng, Chen. Evaluation and compensation of kinematic error to enhance prepolishing accuracy for large aspheric surfaces by robotic bonnet technology. Optics Express (2020)28.
[51] Zhong, Deng, Chen, Zheng. Precision manufacture of aspheric optics by robot-based bonnet polishing. Target Recognition and Artificial Intelligence Summit Forum (2020).
[52] Qin, Liu, Liu. Research on collision detection algorithm of multi-robot bonnet polishing system. Xiamen Univ. of Technology (China);Fudan Univ. (China);Univ. of Shanghai for Science and Technology (China);Univ. of Strathclyde (United Kingdom) (2020).
[53] Ji, Zhang, Yuan, Jin, Yuan. A novel ballonet polishing tool and its robot control system for polishing the curved surface of mould. Int. J. of Computer Applications in Technology (2007)29.
[54] Chen, Miao, Tang, Yin. A review on recent advances in machining methods based on abrasive jet polishing (AJP). International Journal of Advanced Manufacturing Technology (2016)90, 1-15.
[55] Fahnle, Brug, Frankena. Fluid jet polishing of optical surfaces. Applied Optics (1998)37.
[56] Wang, Cheung, Ho, Loh. An Investigation of Effect of Stand-Off Distance on the Material Removal Characteristics and Surface Generation in Fluid Jet Polishing. Nanomanufacturing and Metrology (2020)3.
[57] Wang, Cheung, Ho, Liu, Lee. A novel multi-jet polishing process and tool for high-efficiency polishing. International Journal of Machine Tools and Manufacture (2017)115.

[58] Cheung, Wang, Ho, Chen. Curvature-adaptive multi-jet polishing of freeform surfaces. CIRP Annals (2018)67, 357-360.
[59] Lv, Hou, Tian, Huang, Zhu. Investigation on flow field of ultrasonic-assisted abrasive waterjet using CFD with discrete phase model. Springer London (2018)96.
[60] Hou, Huang, Zhu, Liu, Zou. Study of the Floor Typed Abrasive Water Jet Spatial Machining Robot. Key Engineering Materials (2011)1371.
[61] Wang, Zhu, Huang, Wang, Yao, Zhang. A Study on Erosion of Alumina Wafer in Abrasive Water Jet Machining. Advanced Materials Research (2014)1017, 228-233.
[62] Wang, Zhu, Huang, Wang, Yao. A Study on Ultrasonic Torsional Vibration-Assisted Abrasive Waterjet Polishing of Ceramic Materials. Advanced Materials Research (2016)4231.
[63] Golini, Kordonski, Dumas, Hogan. Magnetorheological finishing (MRF) in commercial precision optics manufacturing. Proceedings of SPIE - The International Society for Optical Engineering (1999)3782.
[64] Jacobs, Golini, Hsu, Puchebner, Strafford, Prokhorov, Fess, Pietrowski, Kordonski. Magnetorheological finishing: a deterministic process for optics manufacturing. In Proceedings of International Conference on Optical Fabrication and Testing.
[65] Harris. History of magnetorheological finishing. Window and Dome Technologies and Materials XII (2011).
[66] Zhang, Li, Xue, Song, Ai. Development and Application of MRF Based on Robot Arm. EPJ Web of Conferences (2019)215.
[67] Li, Zhang, Song, Zhang, Yin, Xue. New generation magnetorheological finishing polishing machines using robot arm. Applied Optics and Photonics China (2019).
[68] Kim, Burge. Rigid conformal polishing tool usingnon-linear visco-elastic effect. Optics Express (2010)18, 2242-2257.
[69] Li, Walker, Zheng, Yu, Reynolds, Zhang, Li. Advanced techniques for robotic polishing of aluminum mirrors. In Proceedings of Optical Fabrication, Testing, and Metrology VI.
[70] Li, Walker, Zheng, Su, Wu, Reynolds, Yu, Li, Zhang. Mid-spatial frequency removal on aluminum free-form mirror. Opt Express (2019)27, 24885-24899.
[71] Zhang, Liu, Yang. Trajectory planning of robot-assisted abrasive cloth wheel polishing blade based on flexible contact. The International Journal of Advanced Manufacturing Technology (2022).
[72] Wang, Yao, Xu, Wu, Shen, sun. Alleviation of honeycomb print-through of NiP/Cu coated carbon fiber composite mirror via robot-arm wheel polishing. Materials Chemistry and Physics (2022)283, 126028.
[73] Guo, Shi, Chen, Yu, Zhao, Shirinzadeh. Optimal Parameter Selection in Robotic Belt Polishing for Aeroengine Blade Based on GRA-RSM Method. Symmetry (2019)11.
[74] Xiao, Huang, Yin. An integrated polishing method for compressor blade surfaces. The International Journal of Advanced Manufacturing Technology (2017)88.
[75] Zc, Fxa, Xjla, Jw, Hn. Design of the parallel mechanism for a hybrid mobile robot in wind turbine blades polishing. Robotics and Computer-Integrated Manufacturing)61.
[76] Preston. The Theory and Design of Plate Glass Polishing Machines. J.soc.glass Tech (1927).
[77] Niwa, Ogawa, Hirogaki, Aoyama, Onchi. Influence of Polishing and Pressing Force on the Material Removal Rate in Fixed Abrasive Polishing with Compact Robot. Advanced Materials Research (2012)565, 243-248.
[78] Zhang, Tam, Yuan, Chen, Zho. An investigation of material removal in polishing with fixed abrasives. Proceedings of the Institution of Mechanical Engineers Part B Journal of Engineering Manufacture

(2002)216, 103-112.
[79] Wan, Zhang, Wang, Xu. Effect of pad wear on tool influence function in robotic polishing of large optics. The International Journal of Advanced Manufacturing Technology (2019).
[80] Jin, Ji, Zhang, Yuan, Zhang, Zhang. Material Removal Model and Contact Control of Robotic Gasbag Polishing Technique. In Proceedings of IEEE Conference on Robotics, Automation & Mechatronics.
[81] Dong, Shi, Liu, Yu. Research of Pneumatic Polishing Force Control System Based on High Speed On/off with PWM Controlling. Robotics and Computer-Integrated Manufacturing (2021)70.
[82] Zhou, Zhao, Tao, Ding. Time-varying isobaric surface reconstruction and path planning for robotic grinding of weak-stiffness workpieces. Robotics and Computer-Integrated Manufacturing (2020)64.
[83] Li, Zhang, Liu, Guan, Wang. A Survey of Robotic Polishing. In Proceedings of 2018 IEEE International Conference on Robotics and Biomimetics (ROBIO).
[84] Ang, Andeen. Specifying and achieving passive compliance based on manipulator structure. Robotics and Automation, IEEE Transactions on (1995)11, 504-515.
[85] Zhang, Zhang, Jiang, Yang, Zhang. Overview of Robot Force Controlled End Effector. Chinese Journal of Engineering Design (2018)25, 617-629.
[86] Wei, Xu. Design of a new passive end-effector based on constant-force mechanism for robotic polishing. Robotics and Computer-Integrated Manufacturing (2022)74.
[87] Du, Sun, Feng, Xu. Automatic robotic polishing on titanium alloy parts with compliant force/position control. Proceedings of the Institution of Mechanical Engineers, Part B: Journal of Engineering Manufacture (2015)229, 1180-1192.
[88] Mohammad, Hong, Wang. Design of a force-controlled end-effector with low-inertia effect for robotic polishing using macro-mini robot approach. Robotics and Computer-Integrated Manufacturing (2018)49, 54-65.
[89] Mizugaki, Sakamoto, Kamijo, Taniguchi. Development of Metal-Mold Polishing Robot System with Contact Pressure Control Using CAD/CAM Data. CIRP Annals (1990)39, 523-526.
[90] Mohammad, Wang. A novel mechatronics design of an electrochemical mechanical end-effector for robotic-based surface polishing. In Proceedings of IEEE/SICE International Symposium on System Integration.
[91] Mohammad, Hong, Wang, Guan. Synergistic integrated design of an electrochemical mechanical polishing end-effector for robotic polishing applications. Robotics and Computer Integrated Manufacturing (2019)55.
[92] Mohammad, Wang. Electrochemical mechanical polishing technology: recent developments and future research and industrial needs. International Journal of Advanced Manufacturing Technology (2016).
[93] Chen, Zhao, Li, Chen, Tan, Ding. Contact force control and vibration suppression in robotic polishing with a smart end effector. Robotics and Computer-Integrated Manufacturing (2019)57, 391-403.
[94] Wang, Wang, Zheng, Yun. Force control-based vibration suppression in robotic grinding of large thin-wall shells - ScienceDirect. Robotics and Computer-Integrated Manufacturing)67.
[95] Huang, Gong, Chen, Zhou. Robotic grinding and polishing for turbine-vane overhaul. Journal of Materials Processing Technology (2002)127, 140-145.
[96] Furukawa, Rye, Dissanayake, Barratt. Automated polishing of an unknown three-dimensional surface. Robotics and Computer-Integrated Manufacturing (1996)12, 261–270.
[97] Brecher, Tuecks, Zunke, Wenzel. Development of a force controlled orbital polishing head for free form surface finishing. Production Engineering (2010)4, 269-277.

[98] Wu, Huang, Wan, Liu, Chen. A Novel Force-Controlled Spherical Polishing Tool Combined With Self-Rotation and Co-Rotation Motion. IEEE Access (2020)8, 108191-108200.

[99] Wahjudi, Shiou. Surface Finish Improvement of Medium-Sized Mold Steel Using an Innovative Sphere-Like Polishing Tool with Force Control. Computer-Aided Design and Applications (2012)9, 621-630.

[100] Xu, Chen, Zhu, Yan, Ding. Hybrid active/passive force control strategy for grinding marks suppression and profile accuracy enhancement in robotic belt grinding of turbine blade. Robotics and Computer-Integrated Manufacturing (2021)67.

[101] Bicchi. Intrinsic contact sensing for soft fingers. In Proceedings of Robotics and Automation, 1990. Proceedings., 1990 IEEE International Conference on.

[102] Shetty, Ang. Active compliance control of a PUMA 560 robot. In Proceedings of IEEE International Conference on Robotics & Automation.

[103] Zeng, Hemami. An overview of robot force control. Robotica (1997)15, 473-482.

[104] Haibo, Shitai, Guilian, Yuxin, Zhenzhong. A hybrid control strategy for grinding and polishing robot based on adaptive impedance control. Advances in Mechanical Engineering (2021)13.

[105] Nagataa, Haseb, Hagab, Omotob, Watanabe. CAD/CAM-based position/force controller for a mold polishing robot. Mechatronics (2007)17, 207-216.

[106] Ding, Min, Fu, Liang. Research and application on force control of industrial robot polishing concave curved surfaces. Proceedings of the Institution of Mechanical Engineers, Part B: Journal of Engineering Manufacture (2018)233, 1674-1686.

[107] Dong, Ren, Hu, Wu, Chen. Contact force detection and control for robotic polishing based on joint torque sensors. The International Journal of Advanced Manufacturing Technology (2020)107, 2745-2756.

[108] Solanes, Gracia, Muñoz-Benavent, Miro, Perez-Vidal, Tornero. Robust Hybrid Position-Force Control for Robotic Surface Polishing. Journal of Manufacturing Science and Engineering (2018)141, 011013.

[109] Lee, Go, Lee, Jun, Kim, Cha, Ahn. A robust trajectory tracking control of a polishing robot system based on CAM data. Robotics and Computer Integrated Manufacturing (2001)17.

[110] Lakshminarayanan, Kana, Mohan, Manyar, Then, Campolo. An adaptive framework for robotic polishing based on impedance control. The International Journal of Advanced Manufacturing Technology (2020), 1-17.

[111] Kana, Lakshminarayanan, Mohan, Campolo. Impedance controlled human–robot collaborative tooling for edge chamfering and polishing applications. Robotics and Computer-Integrated Manufacturing (2021)72, 102199.

[112] Ochoa, Cortesao. Impedance Control Architecture for Robotic-Assisted Mold Polishing based on Human Demonstration. IEEE Transactions on Industrial Electronics (2021), 1-1.

[113] Solanes, Gracia, Muoz-Benavent, Esparza, Miro, Tornero. Adaptive robust control and admittance control for contact-driven robotic surface conditioning. Robotics and Computer-Integrated Manufacturing (2018)54, 115-132.

[114] Guo, Suzuki, Higuchi, Yamagata, Morita. A real-time polishing force control system for ultraprecision finishing of micro-optics. Precision Engineering (2013)37, 787-792.

[115] Wang, Wang. Development of a polishing robot system. In Proceedings of IEEE International Conference on Emerging Technologies & Factory Automation.

[116] Liao, Xi, Liu. Modeling and control of automated polishing/deburring process using a dual-purpose compliant toolhead. International Journal of Machine Tools and Manufacture (2008)48, 1454-1463.

[117] Feng-Yi, Li-Chen. Intelligent robot deburring using adaptive fuzzy hybrid position/force control. IEEE Transactions on Robotics and Automation (2000)16, 325-335.

[118] Zhan, Yu. Study on error compensation of machining force in aspheric surfaces polishing by profile-adaptive hybrid movement–force control. The International Journal of Advanced Manufacturing Technology (2010)54, 879-885.

[119] Minami, Asakura, Dong, Huang. Position control and explicit force control of constrained motions of a manipulator for accurate grinding tasks. Advanced Robotics (1996).

[120] Thomessen, Lien, Sannæs. Robot control system for grinding of large hydro power turbines. Industrial Robot: An International Journal (2001)28, 328-334.

[121] Roswell, Xi, Liu. Modelling and analysis of contact stress for automated polishing. International Journal of Machine Tools and Manufacture (2006)46, 424-435.

[122] Tsai, Huang, Kao. Robotic polishing of precision molds with uniform material removal control. International Journal of Machine Tools and Manufacture (2009)49, 885-895.

[123] Wan, Shi, Yuan, Wu. Research on middle and high spatial-frequency errors by discrete particles abrasion. In Proceedings of 5th International Symposium on Advanced Optical Manufacturing and Testing Technologies: Advanced Optical Manufacturing Technologies.

[124] Tian, Li, Lv, Liu. Polishing pressure investigations of robot automatic polishing on curved surfaces. The International Journal of Advanced Manufacturing Technology (2016)87, 639-646.

[125] Jin, Ji, Pan, Ao, Han. Effect of downward depth and inflation pressure on contact force of gasbag polishing. Precision Engineering (2017)47.

[126] Shibuya, Issiki. Evaluation of Metallic Mold Surfaces Polished by an Industrial Robot with Stick Whetstones. International journal of automation technology (2014)8, 253-263.

[127] Sharma, Shirwalkar, Das, Pal. Robotic polishing of pilger-die. Proceedings of the 2015 Conference on Advances In Robotics - AIR '15 (2015).

[128] Roth, B. W. Mooring, Ravani. An overview of robot calibration. Information Technology Journal (1987)3, 377-385.

[129] Renders, Rossignol, Becquet, Hanus. Kinematic calibration and geometrical parameter identification for robots. Robotics and Automation, IEEE Transactions on (1991)7, 721-732.

[130] Elatta, Gen, Zhi, Daoyuan, Fei. An overview of robot calibration. Information Technology Journal (2004)3, 74-78.

[131] Meggiolaro, Dubowsky, Mavroidis. Geometric and elastic error calibration of a high accuracy patient positioning system. Mechanism and Machine Theory (2004)40.

[132] Gong, Yuan, Ni. Nongeometric error identification and compensation for robotic system by inverse calibration. International Journal of Machine Tools and Manufacture (2000)40.

[133] Zhang, Wang, Zhang, Gan. Machining with flexible manipulator: Toward improving robotic machining performance. In Proceedings of Advanced Intelligent Mechatronics. Proceedings, 2005 IEEE/ASME International Conference on.

[134] Kim, Nam, Ha, Hwang, Lee, Park, Min. Robotic Machining: A Review of Recent Progress. International Journal of Precision Engineering and Manufacturing (2019)20, 1629-1642.

[135] Hwang, Kim, Choi, Shin, Han. Design optimization method for 7 DOF robot manipulator using performance indices. International Journal of Precision Engineering & Manufacturing (2017)18, 293-299.

[136] Denavit, Hartenberg. A Kinematic Notation for Lower-Pair Mechanisms. ASME Journal of Applied

Mechanics (1955)22, 215-221.
[137] Hayati. Robot arm geometric link parameter estimation. In Proceedings of IEEE Conference on Decision & Control.
[138] Judd, Knasinski. A technique to calibrate industrial robots with experimental verification. IEEE Transactions on Robotics and Automation (1987)6, 20-30.
[139] Stone, Sanderson. Statistical performance evaluation of the S-model arm signature identification technique. Proceedings. 1988 IEEE International Conference on Robotics and Automation (1988)10.1109/ROBOT.1988.12180.
[140] Okamura, Park. Kinematic calibration using the product of exponentials formula. Robotica (1996)14.
[141] He, Zhao, Yang, Yang. Kinematic-parameter identification for serial-robot calibration based on POE formula. IEEE Transactions on Robotics (2010)26, 411-423.
[142] Cho, Do, Cheong. Screw based kinematic calibration method for robot manipulators with joint compliance using circular point analysis. Robotics and Computer Integrated Manufacturing (2019)60.
[143] Zhouxiang, Min, Xiaoqi, Yixuan. A new calibration method for joint-dependent geometric errors of industrial robot based on multiple identification spaces. Robotics and Computer-Integrated Manufacturing (2021)71.
[144] Goswami, Quaid, Peshkin. Identifying Robot Parameters Using Partial Pose Information. IEEE control systems (1993)13, 6-14.
[145] Huang, Hong, Mei. Kinematic Calibration of the 3-DOF Module of a 5-DOF Reconfigurable Hybrid Robot using a Double-Ball-Bar System. In Proceedings of IEEE/RSJ International Conference on Intelligent Robots & Systems.
[146] Nubiola, Bonev. Absolute robot calibration with a single telescoping ballbar. Precision Engineering (2014)38, 472-480.
[147] Driels, Swayze, Potter. Full-pose calibration of a robot manipulator using a coordinate-measuring machine. International Journal of Advanced Manufacturing Technology (1993)8, 34-41.
[148] Cong, Yu, Han. Kinematic Calibration of Parallel Robots Using CMM. In Proceedings of Intelligent Control and Automation, 2006. WCICA 2006. The Sixth World Congress on; pp. 8514-8518.
[149] Driels, Pathre. Vision-based automatic theodolite for robot calibration. IEEE Trans. Robotics and Automation (1991)7.
[150] J. Fraczek, Z. Busko. Calibration of multi-robot system without and under load using electronic theodolites. In Proceedings of Robot Motion and Control, 1999. RoMoCo '99. Proceedings of the First Workshop on; pp. 71-75.
[151] Nubiola, Bonev. Absolute calibration of an ABB IRB 1600 robot using a laser tracker. Robotics and Computer Integrated Manufacturing (2013)29.
[152] Zhang, Song, Yang, Pan. Stereo vision based autonomous robot calibration. Robotics and Autonomous Systems (2017)93.
[153] Du, Zhang. Online robot calibration based on vision measurement. Robotics and Computer Integrated Manufacturing (2013)29.
[154] Levenberg. A method for the solution of certain non-linear problems in least squares. Quarterly of Applied Mathematics (1944)2.
[155] Zhou, Kang. A hybrid least-squares genetic algorithm–based algorithm for simultaneous identification of geometric and compliance errors in industrial robots. Advances in Mechanical Engineering (2015)7.

[156] Martinelli, Tomatis, Siegwart. Simultaneous localization and odometry self calibration for mobile robot. Autonomous Robots (2007)22.

[157] Du, Zhang. Online Serial Manipulator Calibration Based on Multisensory Process Via Extended Kalman and Particle Filters. IEEE Transactions on Industrial Electronics (2014)61, 6852-6859.

[158] Nguyen, Zhou, Kang. A calibration method for enhancing robot accuracy through integration of an extended Kalman filter algorithm and an artificial neural network. Neurocomputing (2015)151, 996-1005.

[159] Moré. The Levenberg-Marquardt algorithm: Implementation and theory. Lecture Notes in Mathematics (1978)630.

[160] Qi, Ping, Liu, Jiang. Robot Error Compensation Method Based on Plane Constraint. Journal of Machine Design (2017)34, 23-27.

[161] L.Yu, Liang, W.Qiang, Jiang. Improvement on Robots Positioning Accuracy Based on Genetic Algorithm. In Proceedings of Computational Engineering in Systems Applications, IMACS Multiconference on.

[162] DeVlieg, Szallay. Improved Accuracy of Unguided Articulated Robots. Electroimpact, Inc.;Northrop Grumman Co. (2009).

[163] Devlieg, Szallay. Applied Accurate Robotic Drilling for Aircraft Fuselage. Electroimpact Inc.;Northrop Grumman Corp. (2010).

[164] Veitschegger, Wu. Robot calibration and compensation. IEEE Journal of Robotics and Automation (1988)4, P.643-656.

[165] Zhong, Lewis, N-Nagy. Inverse robot calibration using artificial neural networks. Engineering Applications of Artificial Intelligence (1996)9, 83-93.

[166] Takanashi. 6 DOF manipulators absolute positioning accuracy improvement using a neural-network. In Proceedings of IEEE International Workshop on Intelligent Robots & Systems 90 Towards A New Frontier of Applications.

[167] Zeng, Tian, Liao. Positional error similarity analysis for error compensation of industrial robots. Robotics and Computer Integrated Manufacturing (2016)42.

[168] Tian, Mei, Li, Zeng, Hong, Zhou. Determination of optimal samples for robot calibration based on error similarity. Chinese Journal of Aeronautics (2015)28, 946-953.

[169] Huang, Xiangfei, Kedi, Han. A contour error definition, estimation approach and control structure for six-dimensional robotic machining tasks. Robotics and Computer-Integrated Manufacturing (2022)73.

[170] Ma, Bazzoli, Sammons, Landers, Bristow. Modeling and calibration of high-order joint-dependent kinematic errors for industrial robots. Robotics and Computer Integrated Manufacturing (2018)50.

[171] Luo, Zou, Wang, Lv, Ou, Huang. A novel kinematic parameters calibration method for industrial robot based on Levenberg-Marquardt and Differential Evolution hybrid algorithm. Robotics and Computer-Integrated Manufacturing (2021)71.

[172] Huang, Zhao, Yin, Tian, G. Kinematic calibration of a 6-DOF hybrid robot by considering multicollinearity in the identification Jacobian. Mechanism and Machine Theory (2018)131.

[173] Zhao, Dong, Guo, Tian, Ferrara. Kinematic Calibration Based on the Multicollinearity Diagnosis of a 6-DOF Polishing Hybrid Robot Using a Laser Tracker. Mathematical Problems in Engineering (2018)2018.

[174] Joubair, Bonev. Non-kinematic calibration of a six-axis serial robot using planar constraints. Precision Engineering (2015)40, 325-333.

[175] Jiang, Yu, Jia, Zhao, Xia. Absolute Positioning Accuracy Improvement in an Industrial Robot. Sensors (2020)20.

[176] Chen, Zhang, Sun. Non-kinematic calibration of industrial robots using a rigid–flexible coupling error model and a full pose measurement method. Robotics and Computer-Integrated Manufacturing (2019)57.

[177] Yuan, Pan, Ding, Sun, Li. A Review on Chatter in Robotic Machining Process Regarding Both Regenerative and Mode Coupling Mechanism. IEEE/ASME Transactions on Mechatronics (2018)23, 2240-2251.

[178] Huang, He, Xiao, Li, Jiahua, Wang. Effects research on theoretical-modelling based suppression of the contact flutter in blisk belt grinding. Journal of Manufacturing Processes (2020)54.

[179] Pan, Zhang, Zhu, Wang. Chatter analysis of robotic machining process. Journal of Materials Processing Technology (2006).

[180] Moradi, Bakhtiari-Nejad, Movahhedy. Tuneable vibration absorber design to suppress vibrations: An application in boring manufacturing process. Journal of Sound and Vibration (2008)318, 93-108.

[181] Quintana, Ciurana. Chatter in machining processes: A review. International Journal of Machine Tools & Manufacture (2011)51, 363-376.

[182] S.Sharnappa, N, Sethuraman. Buckling and free vibration analysis of magnetic constrained layer damping (MCLD) beam. Finite Elements in Analysis & Design (2009)45, 156-162.

[183] Morita, Kimata, Ukai, Kando. Lyapunov-based control of macro-micro manipulator considering bending and torsional vibrations. In Proceedings of International Workshop on Robot Motion & Control.

[184] Ge, Tee, IvanE.Vahhi, FrancisE.H.Tay. Tracking and Vibration Control of Flexible Robots Using Shape Memory Alloys. IEEE/ASME Transactions on Mechatronics (2006)11, 690-698.

[185] Kiang, Spowage, Yoong. Review of Control and Sensor System of Flexible Manipulator. Journal of Intelligent & Robotic Systems (2015)77.

[186] Qiu, Li. Active Vibration Control and Experiment of Two-Link Flexible Manipulator. Journal of Vibration,Measurement & Diagnosis (2019)39, 503-511+668.

[187] Zou, Qu, Xu. A symmetric S-curve Trajectory Planning for Robot Point-to-point Motion. In Proceedings of 2009 IEEE International Conference on Robotics and Biomimetics, Guilin; pp. 2172-2176.

[188] Ji, Lei, Ji, Lu, Gao. An adaptive real-time NURBS curve interpolation for 4-axis polishing machine tool. Robotics and Computer Integrated Manufacturing: An International Journal of Manufacturing and Product and Process Development%J (2021)67.

[189] Ho, Tu. Position control of a single-link flexible manipulator using H∞-based PID control. IEE Proceedings -- Control Theory & Applications (2006)153, 615-622.

[190] Lochan, Roy, Subudhi. Robust tip trajectory synchronisation between assumed modes modelled two-link flexible manipulators using second-order PID terminal SMC. Robotics and Autonomous Systems (2017), 108-124.

[191] Waweru, Minoru, Kojiro. Gain Tuning for High-Speed Vibration Control of a Multilink Flexible Manipulator Using Artificial Neural Network. Journal of Vibration and Acoustics (2019)141.

[192] Qiu, Li, Zhang. Experimental study on active vibration control for a kind of two-link flexible manipulator. Mechanical Systems and Signal Processing (2019)118.

[193] Dubay, Hassan, Li, Charest. Finite element based model predictive control for active vibration suppression of a one-link flexible manipulator. Isa Trans (2014)53, 1609-1619.

[194] Arakelian. Gravity compensation in robotics. Advanced Robotics (2015)30, 79-96.

[195] Tian, Lv, Li, Liu. Modeling and control of robotic automatic polishing for curved surfaces. CIRP Journal of Manufacturing Science and Technology (2016)14, 55-64.

[196] Zhang, Liu, Zang, Li. A hybrid passive/active force control scheme for robotic belt grinding system. In Proceedings of 2016 IEEE International Conference on Mechatronics and Automation.

[197] Gao, Tian, Yang, Li. Research on Platform Construction and Gravity Compensation of Robot Automatic Grinding and Polishing System. Tool Engineering (2015)49, 47-50.

[198] Salisbury. Active stiffness control of a manipulator in cartesian coordinates. 1980 19th IEEE Conference on Decision and Control including the Symposium on Adaptive Processes (1980).

[199] Chen, Kao. Geometrical approach to the conservative congruence transformation (CCT) for robotic stiffness control. In Proceedings of IEEE International Conference on Robotics & Automation.

[200] Alici, Shirinzadeh. Enhanced Stiffness Modeling, Identification and Characterization for Robot Manipulators. IEEE Transactions on Robotics: A publication of the IEEE Robotics and Automation Society (2005)21, 554-564.

[201] Klimchik, Furet, Caro, Pashkevich. Identification of the manipulator stiffness model parameters in industrial environment. Mechanism and Machine Theory: Dynamics of Machine Systems Gears and Power Trandmissions Robots and Manipulator Systems Computer-Aided Design Methods (2015)90, 1-22.

[202] Dumas, Caro, Garnier, Furet. Joint stiffness identification of six-revolute industrial serial robots. Robotics and Computer Integrated Manufacturing (2011)27, 881-888.

[203] Rui, Qiao, Wen, Zhang, Wang. Research on Joint Stiffness Identification and Error Compensation of Serial 6-DOF Robot. Journal of Mechanical Transmission (2019)43, 37-42.

[204] Abele, Weigold, Rothenbücher. Modeling and Identification of an Industrial Robot for Machining Applications. CIRP Annals - Manufacturing Technology (2007)56, 387-390.

[205] Lehmann, Olofsson, Nilsson, Halbauer, Haage, Robertsson, Sörnmo, Berger. Robot Joint Modeling and Parameter Identification Using the Clamping Method. IFAC Proceedings Volumes (2013)46, 813-818.

[206] Guo, Dong, Ke. Stiffness-oriented posture optimization in robotic machining applications. Robotics & Computer Integrated Manufacturing (2015)35, 69-76.